INTERNATIONAL JOURNAL OF
ENERGY AND ENVIRONMENT

Volume 4, Issue 4, 2013 pp.581-614

Journal homepage: www.IJEE.IEEFoundation.org

Comparative evaluation of kinetic, equilibrium and semi-equilibrium models for biomass gasification

Buljit Buragohain[1], Sankar Chakma[2], Peeush Kumar[2], Pinakeswar Mahanta[1,3], Vijayanand S. Moholkar[1,2]

[1] Center for Energy, Indian Institute of Technology Guwahati, Guwahati – 781 039, Assam, India.
[2] Department of Chemical Engineering, Indian Institute of Technology Guwahati, Guwahati – 781 039, Assam, India.
[3] Department of Mechanical Engineering, Indian Institute of Technology Guwahati, Guwahati – 781 039, Assam, India.

Abstract
Modeling of biomass gasification has been an active area of research for past two decades. In the published literature, three approaches have been adopted for the modeling of this process, viz. thermodynamic equilibrium, semi-equilibrium and kinetic. In this paper, we have attempted to present a comparative assessment of these three types of models for predicting outcome of the gasification process in a circulating fluidized bed gasifier. Two model biomass, viz. rice husk and wood particles, have been chosen for analysis, with gasification medium being air. Although the trends in molar composition, net yield and LHV of the producer gas predicted by three models are in concurrence, significant quantitative difference is seen in the results. Due to rather slow kinetics of char gasification and tar oxidation, carbon conversion achieved in single pass of biomass through the gasifier, calculated using kinetic model, is quite low, which adversely affects the yield and LHV of the producer gas. Although equilibrium and semi-equilibrium models reveal relative insensitivity of producer gas characteristics towards temperature, the kinetic model shows significant effect of temperature on LHV of the gas at low air ratios. Kinetic models also reveal volume of the gasifier to be an insignificant parameter, as the net yield and LHV of the gas resulting from 6 m and 10 m riser is same. On a whole, the analysis presented in this paper indicates that thermodynamic models are useful tools for quantitative assessment of the gasification process, while kinetic models provide physically more realistic picture.

Keywords: Biomass gasification, CFB gasifier, equilibrium models, Gibbs energy minimization, Pyrolysis, Producer gas.

1. Introduction

Biomass gasification has emerged as a potential solution to rural electrification in developing countries through decentralized power generation. In addition, being a renewable energy source, biomass gasification also helps reduction of net greenhouse gas emission and mitigation of global warming. Gasifiers of different types and varying capacities are currently available in market. The capacities range from as low as 10 kW to a few MW. Broadly gasifiers are classified as moving bed and fluidized bed. Based on the relative flow of biomass and gasification medium (air), the moving bed gasification are

further categorized as: (i) updraft, (ii) downdraft and (iii) cross draft. On the other hand, the mode of fluidization is used to categorize fluidized bed gasifies as bubbling bed and circulating fluidized bed. An efficient design and scale up of a gasifier requires an insight into the process of gasification through mathematical and physical models. Past 3 decades have seen immense research activity in this field.

Basic chemistry of biomass gasification closely resembles that of coal gasification, and hence, mathematical models for biomass gasification have been derived from coal gasification. However, these are several differences in the composition of biomass and coal. In addition to lignin (as in coal), biomass also contains significant amount of hemi–cellulose and cellulose. The reactivity of biomass is usually much higher than that of coal, which is mainly attributed to very low ash content of biomass. Another important difference is in term of relative contents of volatiles and fixed carbon. The fixed carbon content of coal is much higher than biomass, while volatiles content of biomass is significantly higher than coal. The volatiles released during the pyrolysis of biomass (which occurs at much faster rate than coal) can condense in the form of tar, if the gasification temperature is below ~ 1000^{o}C. Tar content in the producer gas resulting from biomass gasification can create significant operational problems in the equipment (for example, furnace, dual fuel or 100% producer gas engines etc.), in which the gas is used. There have been mainly two approaches adopted by researcher in modeling of biomass gasification. First is that of equilibrium modeling, in which the Gibbs free energy of the gasification system is minimized to determine the composition of the species resulting from gasification of biomass. These models are further classified on the basis of algorithm used for Gibbs energy minimization as stoichiometric and non–stoichiometric models. The stoichiometric models take into account specific chemical reactions and the equilibrium constants of these reactions at gasification temperature. The non–stoichiometric models are based on elemental balance technique, in which the composition of the reaction mixture is determined using Gibbs energy minimization using numerical methods such as Langrangian multipliers. The second approach for modeling of gasifier is kinetic modeling, in which the scheme of reactions occurring during gasification is coupled to hydrodynamics of the gasifier. Among the three approaches, physically most realistic approach is the kinetic modeling. However, many limitations of these models restrict their wide applicability. The first limitation is that of availability of precise kinetic constants over a wide range of temperature and pressure. Second limitation is in terms of coupling of hydrodynamics of the gasifiers and kinetics of reaction scheme by identification and quantification of proper linkages between the two. These models involve various physical aspects of the gasification system such as gas solid and solid–solid (heat and mass) transport coefficients, velocities of various phases and residence time distribution. These features make the model system specific and more error prone. Equilibrium models are on the contrary, independent of design of gasifier. Thus, these can be applied to both moving and fluidized bed gasifiers. In addition, thermodynamic models predict the "limiting" or maximum possible performance of the gasifier under a given set of operating conditions. Thus, predictions of these models form useful basis for optimization of gasifier in terms of operating conditions.

Biomass gasification process essentially aims at selective conversion of biomass to carbon monoxide and hydrogen. The extent of this conversion is a function of both design and operating parameters. Practically, complete conversion of biomass to desired products is not achieved. Some fraction of carbon in the biomass remains unconverted in the form of char, while some carbon appears in the form of tar, which are essentially heavy hydrocarbons (both aliphatic and aromatic) that condense at room temperature. Formation of char and tar is loss of energy of the biomass. Extent of carbon conversion determines the quality (lower heating value, MJ/Nm^3) and quantity (Nm^3 of gas/kg of biomass) of producer gas resulting from gasification. On microscopic level, elemental composition (C, H, N, and O) of gasification mixture determines these parameters. The elemental composition of gasification mixture, in turn, is generated by biomass type, moisture content of the biomass and the equivalence or air ratio.

2. Aim and approach of present study

In this paper, we have attempted to compare the equilibrium, semi–equilibrium and kinetic models of biomass gasification using a circulation fluidized bed gasifier as basis. We have selected two biomass, viz. wood particles (or dust) and rice husk, with gasification medium being air as the model system. The equilibrium model used in our study is based on well known algorithm SOLGASMIX [1]. The elemental vector input to this model is determined from ultimate composition of biomass and the air ratio. This model has also been used to determine semi–equilibrium conditions by using extent of carbon conversion as a manipulation parameter. The kinetic model comprises of scheme of 13 known chemical reactions (both homogeneous and heterogeneous) among various species resulting from pyrolysis of biomass. The

kinetic constants for these reactions have been obtained from literature. Section 4 gives greater details the physical picture of the gasification process in the CFB gasifier. Extent of carbon conversion achieved in the gasifier depends mainly on the temperature and air ratio. It should be noted, however, that temperature of the gasifier itself depends on extent of carbon conversion due to simultaneous endothermic /exothermic reactions during gasification. Thus, in principle carbon conversion can not be considered as an "independent" or manipulation parameter. But, for a CFB gasifier, the extent of carbon conversion also depends on the residence time of biomass particles, which is governed by velocity of these particles. For no slip condition, velocity of the biomass particles is equal to air velocity in the riser section of gasifier, which is a design parameter, as explained in the next section. On the basis of these arguments, the semi–equilibrium model uses carbon conversion as independent parameter. Finally, we have compared the predictions of various models against experimental data.

3. Literature review

Before proceeding to the methodology and results section, we briefly review here the literature in the area of modeling of biomass gasification using both kinetic and equilibrium approaches. Kinetic models are mostly associated with fluidized bed gasifiers, in which the process of gasification is kinetically limited. As far as modeling of fluidized bed gasifiers is concerned, coal gasification has been extensively studied. Some notable contribution to coal gasification are from [2-12]. We would like to specifically mention that literature on coal gasification /combustion in circulating/bubbling fluidized bed is quite vast, and a thorough review of it is beyond the scope of this paper. References cited above are a few representative papers in this area. The models for coal gasification /combustion in fluidized bed systems have formed basis for development of models for biomass gasification. Literature on kinetic modeling of biomass gasification in various types of gasifiers has also seen numerous contributions in last two decades.

Contribution in 1980s are from Belleville and Capart [13], who developed a model to predict outlet gas concentration from wood gasifier, and Chang et al. [14], who developed a model for biomass gasification in fluidized bed. In another notable contribution, van der Aarsen [15] modeled a fluidized bed wood gasifier. Literature published in 1990s includes contribution from Corella et al. [16], who addressed the issue of non–stationary states in a commercial fluidized bed air–biomass gasifier. Jiang and Morey [17,18] have developed a numerical model for fluidized bed biomass gasifier, which was based on their own experiments. Experiments were conducted in lab–scale gasifier–combustion system, with gas samples analyzed using online gas chromatograph.

The numerical model of Jiang and Morey [17,18] was 1–D, steady state comprising of 4 sub–models, viz. fuel pyrolysis model, oxidation model, gasification model and freeboard model. The model could assess major mechanisms of gasification such as fuel pyrolysis and chemical/physical rate processes. Wang and Kinoshita [19] have also developed kinetic model of biomass gasification based on mechanism of surface reaction, in which the approach rate constants were computed by minimizing differences between experimental data and theoretical results. Mansaray et al. [20, 21] have developed two models (single and double compartment) using ASPEN PLUS process simulator that could predict steady state performance of a dual distributor type fluidized bed rice husk gasifier under wide range of operating conditions. Sadaka et al. [22-24] developed a model for bubbling fluidized bed gasifier on the basis of two–phase theory of fluidization. In this model, the fluidized bed was divided in 3 zones and transport co–efficient (heat and mass) were calculated in each zone for both bubble and combustion phase. Other models include those from [25-37].

Numerous authors have applied both stoichiometric and non–stoichoimetric models for biomass gasification. The notable contributions include: [38-45] have assed performance of biomass gasification system for decentralized heat and power generation with equilibrium models, and Zainal et al. [46] have studied effect of gasification temperature and moisture content of biomass on producer gas composition. Similarly, Alderucci [47] has studied gasification of biomass with steam and CO_2 as gasification medium. Ruggerio and Manfrida [48] have also attempted to predict performance of downdraft gasifier (in terms of product gas composition and overall efficiency) using thermodynamic model. Some other studies using equilibrium (or semi–equlibrium) models are from [49-53].

Literature involving application of non–stoichiometric model is relatively less. Researchers have applied different algorithms for Gibbs energy minimization. These algorithms include STANJAN [54], RAND [55] and SOLGASMIX [1]. The major contributions in this area are from [56-59].

For greater details on both equilibrium and kinetic modeling of biomass gasification we refer the reader to state of the art reviews by [60-63].

3.1 Inference and justification of present study

Voluminous literature has been published in the area of modeling of biomass gasification using both kinetic and equilibrium approach. As noted earlier, kinetic models have advantage of being physically more realistic, while equilibrium model have merit of wide applicability and being independent of gasifier design. A comparative study is, thus, necessary to compare the predictions of the two models under same gasification conditions. Such comparison will give quantitative account of the discrepancy in the predictions of the two models. This will help identify suitability of the models under a particular situation. It will also help identify conditions for which and under which the gasification system deviates from equilibrium. Such an analysis will help identify process/design parameters, which play vital role in achieving equilibrium in the system (i.e. conditions for which the output of gasification process will be at its maximum).

4. Physical picture of gasification in a CFB biomass gasifier

We take a typical pilot scale circulating fluidized bed biomass gasifier as basis for comparison of kinetic and equilibrium models. This gasifier unit comprises of: (1) riser, (2) cyclone separator, (3) burner–blower system for hot gas generation, (4) biomass hopper and screw feeder, (5) gas cooling system, (6) particulate filter system (either single or double stage), and (7) dual fuel generator. We briefly describe here the physics or mechanics of the process. Biomass enters the riser section of the gasifier near (just above) the perforated plate distributor. The gasifier medium is hot air at about 700–900^{o}C, and enters from the below the distributor plate. A bed of sand (stagnant height ~ 30 cm) is used as inert material in the riser (ID = 4 in.). Initially, hot air–sand mixture is circulated in the gasifier riser section to establish (almost) uniform temperature in the riser. The velocity of air through riser is so adjusted as to give turbulent or vigorous bubbling mode of fluidization for sand, while pneumatic conveyance regime for biomass particles. Under these fluidization conditions, the bed of sand expands about 50–60% of its initial height. Biomass entering the riser has medium particle size of ~ 0.5 – 1 mm, and gets mixed with hot sand in turbulent motion. Both gas–particle and particle–particle heat transfer rates are high, and hence, biomass particles reach the temperature of sand bed and get pyrolyzed almost instantly. Liu and Gibbs [30] have given following expression for the devolatilization time (in seconds) of biomass particles: $t_d = \frac{27.443 d_p^{1.662}}{(T-613)^{0.508}}$ where d_p is the biomass particle size in mm, and T is the temperature in K. It should be noted that biomass particles may also get ruptured or sintered during mixing with hot sand. We, therefore, have considered a range of particle sizes, viz. 0.5 – 1 mm for our analysis. The pyrolysis time for these particles is ~ 0.13 s and 1.38 s, respectively. This is sufficiently small to justify assumption of instantaneous de-volatilization of biomass particles. Pyrolysis of biomass results in fractionation of biomass into three components: char (which is carbon rich solid fraction), tar (which is essentially heavy hydrocarbons) and light gases such as CO, CO_2, H_2, CH_4, C_2H_4 and C_2H_6.

The products of pyrolysis, viz. char, tar and gases disengage and emerge out of the turbulent sand bed, and flow along the riser with gasification medium; finally exiting at the top to enter a cyclone separator. Various species in the gas undergo reactions during their flow through the riser. These reactions are both heterogeneous (between char and gases) and homogeneous (among gas species) type. The cyclone separator separates the solid from exhaust gas, i.e. char particles and also some sand particles that get elutriated, and return them to the riser bottom. The gas exiting from cyclone separator has fine dust particles (of a size smaller than the critical particle size captured by cyclone separator). This gas in initially cooled by spraying water in it. With cooling of gas at room temperature, the tar component condenses and gets carried in the form of droplets in the gas. The gas is then filtered to remove both solid particles and tar droplets, and also passed through moisture absorber beds (such as saw dust). It is then fired into the producer gas engine coupled to a generator.

5. Model formulation

5.1 Kinetic model

The kinetic model takes into account 13 simultaneous reactions among various species resulting out of pyrolysis. These reactions and their kinetic constants are given in Table 1. The reaction scheme

comprises of 4 heterogeneous reactions of char gasification with O_2, H_2O, CO_2 and H_2. In addition, 9 homogeneous reactions have been considered among 9 species, viz. O_2, CO, CO_2, H_2O, H_2, CH_4, C_2H_6, C_2H_4 and tar. The mole / mass balance for various species is written as:

Carbon: $$\frac{dF_{Char}}{dV}\left(\frac{kg}{m^3-s}\right)=-\frac{1}{uA}\left(r_1+r_2+r_3+r_4\right) \quad (1)$$

Oxygen: $$\frac{dF_{O_2}}{dV}\left(\frac{kmol}{m^3-s}\right)=-\left(\frac{0.85}{12}\right)\frac{r_1}{uA}-0.5r_6-1.5r_7-0.5r_8-0.5r_{10}-r_{11}-3r_{12}-0.68r_{13} \quad (2)$$

Carbon monoxide (CO): $$\frac{dF_{CO}}{dV}\left(\frac{kmol}{m^3-s}\right)=\left(\frac{0.3}{12}\right)\frac{r_1}{uA}+\frac{1}{12}\frac{r_2}{uA}+\left(\frac{2}{12}\right)\frac{r_3}{uA}-r_5-r_6+r_7+r_8+r_9+0.8r_{11}+0.75r_{13} \quad (3)$$

Carbon Dioxide (CO_2): $$\frac{dF_{CO_2}}{dV}\left(\frac{kmol}{m^3-s}\right)=\left(\frac{0.7}{12}\right)\frac{r_1}{uA}-\frac{r_3}{12uA}+r_5+r_6+2r_{12}+0.25r_{13} \quad (4)$$

Water (H_2O): $$\frac{dF_{H_2O}}{dV}\left(\frac{kmol}{m^3-s}\right)=-r_5+2r_7-r_9+r_{10}+1.2r_{11}+2r_{12}+0.28r_{13} \quad (5)$$

Hydrogen (H_2): $$\frac{dF_{H_2}}{dV}\left(\frac{kmol}{m^3-s}\right)=\frac{r_{12}}{12uA}-\left(\frac{2}{12}\right)\frac{r_4}{uA}+r_5+2r_8-3r_9-r_{10} \quad (6)$$

Methane (CH_4): $$\frac{dF_{CH_4}}{dV}\left(\frac{kmol}{m^3-s}\right)=\frac{r_4}{12uA}-r_7-r_8-r_9 \quad (7)$$

Ethane (C_2H_6): $$\frac{dF_{C_2H_6}}{dV}\left(\frac{kmol}{m^3-s}\right)=-0.04r_{11} \quad (8)$$

Ethylene (C_2H_4): $$\frac{dF_{C2H4}}{dV}\left(\frac{kmol}{m^3-s}\right)=-r_{12} \quad (9)$$

Tar: $$\frac{dF_{Tar}}{dV}\left(\frac{kmol}{m^3-s}\right)=-r_{13} \quad (10)$$

The term (uA) is the instantaneous volume of the reaction mixture and a factor that converts the original rate expression for char gasification in kg/s to kg/m^3–s. It has been derived with simple chain rule as follows:

$$\frac{dW}{dV}\left(\frac{kg}{m^3-s}\right)=\frac{dW}{dt}\times\frac{dt}{dV}=\frac{r_1}{A}\times\left(\frac{dt}{dx}\right)=\frac{r_1}{uA} \quad (11)$$

dV is the differential volume of the gasification mixture. Since the gasification mixture flows axially through the riser, we can represent the differential volume of thickness dx as $A \times dx$, where A is the area of cross–section. dx/dt is the axial velocity (u) of the gasification mixture (char + tar + gaseous species). Assuming no slip condition in the gasification mixture, i.e. the solid char particles move with same velocity as the gasification mixture, the velocity can be calculated by dividing the volume of the gaseous species in the mixture by the cross–sectional area of riser. The above reaction scheme is integrated with volume as an independent variable with Runge–Kutta 4th order – 5th order adaptive step size method. We consider two heights for the riser section, viz. 6 and 10 m. The corresponding volumes of the risers (for 4" ID) are 0.0486 and 0.081 m^3, respectively.

Table 1. Scheme of reactions in the kinetic model along with rate expressions

Sr. No.	Reaction	Rate Expression (either kg/s or kmol/m^3-s, as applicable)	References
		Heterogeneous Reactions of Char Gasification	
1.	$(1+\beta_c)\,C+\left(1+\frac{\beta_c}{2}\right)O_2 \longrightarrow \beta_c\,CO+CO_2$ $C+0.85O_2 \longrightarrow 0.3CO+0.7CO_2$	$r_1=-\frac{dW}{dt}=2.268\times10^7\times\exp\left(\frac{-8559}{T}\right)W_p[O_2]$ (kg/s) $(\beta_c=0.43)$	[6, 29, 30, 88]
2.	$C+H_2O \longrightarrow CO+H_2$	$r_2=-\frac{dW}{dt}=\frac{6692\times\exp\left(\frac{-15516}{T}\right)\times W_p\times[H_2O]}{1+3.16\times10^{-2}\exp\left(\frac{3620}{T}\right)[H_2O]+5.36\times10^{-3}\exp\left(\frac{7193}{T}\right)\times[H_2]+8.25\times10^{-5}\exp\left(\frac{11559}{T}\right)[CO]}$ (kg/s)	[87]
3.	$C+CO_2 \longrightarrow 2\,CO$	$r_3=-\frac{dW}{dt}=\frac{1.3692\times10^0\left(\frac{-32235}{T}\right)\times W_p\times[CO_2]}{1+6.6\times10^{-2}[CO_2]+0.12\exp\left(\frac{3067}{T}\right)\times[CO]}$ (kg/s)	[87]
4.	$C+2\,H_2 \longrightarrow CH_4$	$r_4=-\frac{dW}{dt}=\frac{66.92\times\exp\left(\frac{-15516}{T}\right)\times[H_2]\times W_p}{1+3.16\times10^{-2}\exp\left(\frac{3620}{T}\right)[H_2O]+5.36\times10^{-3}\exp\left(\frac{7193}{T}\right)\times[H_2]+8.25\times10^{-5}\exp\left(\frac{11559}{T}\right)[CO]}$ (kg/s)	[30]
		Homogeneous Reaction among Gaseous Species	
5.	$CO+H_2O \rightleftharpoons CO_2+H_2$	$r_5=\frac{-d[CO]}{dt}=2.78\times10^3\times\exp\left(\frac{-1510.7}{T}\right)\left[[CO][H_2O]-\frac{[CO_2][H_2]}{0.0265\exp\left(\frac{3958.5}{T}\right)}\right]$ (kmol/m^3-s)	[89, 90]
6.	$CO+0.5\,O_2 \longrightarrow CO_2$	$r_6=\frac{-d[CO]}{dt}=3.25\times10^{10}\exp\left(\frac{-15098}{T}\right)\left[[CO][O_2]^{1/2}[H_2O]^{1/2}\right]$ (kmol/m^3-s)	[91]
7.	$CH_4+\frac{3}{2}\,O_2 \longrightarrow CO+2\,H_2O$	$r_7=\frac{-d[CH_4]}{dt}=5\times10^{11}\exp\left(\frac{-24157}{T}\right)[CH_4]^{0.7}[O_2]^{0.8}$ (kmol/m^3-s)	[91]
8.	$CH_4+\frac{1}{2}\,O_2 \longrightarrow CO+2\,H_2$	$r_8=\frac{-d[CH_4]}{dt}=4.4\times10^{11}\exp\left(\frac{-15098}{T}\right)[CH_4]^{1/2}[O_2]^{5/4}$ (kmol/m^3-s)	[92]
9.	$CH_4+H_2O \longrightarrow CO+3\,H_2$	$r_9=\frac{-d[CH_4]}{dt}=3\times10^8\times\exp\left(\frac{-15098}{T}\right)[CH_4][H_2O]$ kmol/m^3-s	[92, 93]
10.	$H_2+\frac{1}{2}O_2 \longrightarrow H_2O$	$r_{10}=\frac{-d[H_2]}{dt}=5.183\times10^{13}T^{3/2}\exp\left(\frac{-3420}{T}\right)[H_2]^{3/2}[O_2]$	[92]
11.	$C_2H_6+\frac{5}{2}\,O_2 \longrightarrow 2\,CO+3\,H_2O$	$r_{11}=\frac{-d[O_2]}{dt}=2.281\times10^{11}\exp\left(\frac{-20131}{T}\right)T^{0.5}[C_nH_m][O_2]$	[94]
12.	$C_2H_4+3\,O_2 \longrightarrow 2\,CO_2+2\,H_2O$	$r_{12}=\frac{-d[C_2H_4]}{dt}=4\times10^{11}\exp\left(\frac{-24200}{T}\right)[C_2H_4]^{0.7}[O_2]^{0.8}$	[28, 95]
13.	$CH_{0.85}O_{0.17}$ (Tar) $+0.68\,O_2 \longrightarrow$ $0.75\,CO+0.25\,CO_2+0.28\,H_2O$	$r_{13}=\frac{-d[Tar]}{dt}=1.264\times10^{13}\exp\left(\frac{-24200}{T}\right)[Tar][O_2]$	[28]

5.2 Equilibrium model

The equilibrium model is based on algorithm SOLGASMIX proposed by Eriksson [1] for calculation composition of reaction system at thermodynamic equilibrium through Gibbs energy minimization of the system. Simulations have been carried out with software FACTSAGE [64, 65]. We give below only the main equations of this model. For greater details on the model, please refer to original paper by Eriksson [1] or earlier paper by authors of this study [66]. Solution to this model is obtained using an iterative procedure (method of Lagrangian multipliers with constraint of mass balance equations) in terms of mole numbers and fractions of gas / condensed phase species at equilibrium that could result from reactant species at a specific temperature and pressure, for which the total free energy of the system is at its minimum.

Total Gibbs free energy (G) of a system comprising of mixture of *i* species is:

$$G=\sum_i x_i g_i \tag{12}$$

x_i is the mole number of a substance or species in the mixture. Chemical potential of a species *i* (g_i) is:

$$g_i=g_i^0+RT\ln a_i \tag{13}$$

a_i represents activity coefficient of a species and it is equal to the partial pressure p_i for a gaseous species assuming ideal behavior:

$$a_i = p_i = (x_i / X)P \tag{14}$$

X represents total number of moles in the gas phase and *P* is the total pressure of the system, respectively. The condensed substances are assumed to be pure, and hence, their activities are equal to unity. With these assumptions, a new dimensionless quantity (*G/RT*) is defined as:

$$G/RT = \sum_{i=1}^{m} x_i^g [(g^0/RT)_i^g + \ln P + \ln(x_i^g / X)] + \sum_{i=1}^{s} x_i^c (g^0/RT)_i^c \tag{15}$$

Superscripts *g* and *c* represent gas phase and condensed phase, respectively, while *m* and *s* represent the total number of substances in the gas phase and condensed phase, respectively, at equilibrium. *R* is the ideal gas constant. The quantity (g^o/RT) for a certain substance is calculated as with reference to standard state at 298 K:

$$(g^o/RT) = (1/R)[G^o - H_{298}^o)/T + \Delta_f H_{298}^o / RT \tag{16}$$

Superscript ^{o} refers to the thermodynamic standard state; subscript $_{298}$ refers to the reference temperature; subscript $_f$ denotes the formation of a compound from the elements in their standard states. Overall mass balance in the system among various species can be written as:

$$\sum_{i=1}^{m} a_{ij}^g x_i^g + \sum_{i=1}^{s} a_{ij}^c x_i^c = b_j \, (j = 1, 2, ...l) \tag{17}$$

Various notations are as follows: a_{ij} – number of atoms of the j^{th} element in a molecule of the i^{th} substance, b_j – total number of moles of the j^{th} element, l – total number of elements. The method involves a. For solution of this system of equations, Lagrange's method of undetermined multipliers is used. The solution essentially involves minimization of the free energy *G* of a system (or equivalently *G/RT* as given in equation 15) subject to the mass balance constraints.

Total heat of the process for attainment of equilibrium is determined as follows:

The energy necessary for pre–heating the initial mixture (*HP*) from the initial temperature T_1 K to the reaction temperature *T* K, added to the heat of reaction (HR), gives the total heat (HT): $HT = HP + HR$. HP and HR are determined as follows:

$$HP = \sum_i x_i^* (H^o - H_{T1}^o)_i \tag{18}$$

where x^* denotes the number of moles in the initial mixture, and:

$$(H^o - H_{T1}^o)_i = \int_{T_1}^{T} (C_p)_i \, dT \tag{19}$$

$$HR = \sum_i (\Delta_f H_T^o)_i (x_i - x_i^*) \tag{20}$$

where, $(\Delta_f H_T^o)_i = (\Delta_f H_{298}^o)_i + [(H^o - H_{298}^o)_i - (H^o - H_{298}^o)_{elements}]$. Various notations are: *H* = enthalpy (heat content); *T* = absolute temperature of the system; x^* = number of moles in the initial mixture; C_p = heat capacity at constant pressure as a function of temperature; $\Delta_f H_{298}^o$ = heat of formation at 298.15 K; $\left(G^o - H_{298}^o\right)/T$ = free energy function; $\left(H^o - H_{298}^o\right)$ = heat content function.

5.3 Simulation parameters for kinetic and equilibrium model

The simulation of gasification using either kinetic or equilibrium model requires 3 important parameters. These are: (i) temperature of gasification, (ii) pressure of gasification, and (iii) type of biomass. We have

chosen values of these parameters on the basis of results of our previous studies, experimental studies published in literature and specifications of commercial gasifiers available in market. For the biomass type, our choice is rice husk and wood particles (or dust). These are most common feedstock used in commercial gasifiers. As far as gasification medium is concerned, we have chosen air for our analysis.

1- Temperature profile

The axial profile of temperature in the riser section is a critical parameter influencing gasification process. The axial profile of temperature, in turn, is affected by several factors such as temperature of incoming gasification medium (air or air–steam mixture), the heat released during gasification, the heat capacity of gasification mixture (sand, char particles and producer gas) and the losses of heat occurring from the riser. The temperature is the highest near the distributor, where the biomass entering the riser mixes with hot and turbulent sand bed and undergoes pyrolysis. The temperature shows a decreasing profile with height of the riser. The kinetic constants of various oxidation / reduction occurring in the riser depend on temperature. As an approximation, we have considered in our analysis an average of typical temperatures at the distributor plate of the riser and exit point of the gasification mixture [67, 68]. We choose two temperatures, viz. 700 and 800^{o}C for our simulations. Another basis for the choice of these temperatures are the results of our previous study, in which we have determined optimum operating conditions for gasification of different biomass. A more rigorous approach in the report would be a step–by–step iterative calculation in which the extent of reaction, heat released /absorbed during reaction, and temperature of the gasifier are calculated in discrete manner.

2- Velocity of air

The superficial velocity of hot air (gasification medium) entering the riser was chosen on the basis of hydrodynamic behavior of sand and biomass particles. We have considered that smooth sand as inert bed material. The particle size of sand is uniformly 270 μm. The minimum fluidization velocity and terminal settling velocity for these particles are 0.028 m/s and 1.45 m/s, respectively. The biomass, on the other hand, undergoes significant particle size reduction after getting pyrolyzed. The char particles emerging out of sand bed have a broad range of size and shape. We have considered 3 sizes of char particles for deciding the superficial velocity of air through the riser. The minimum fluidization velocities and terminal settling velocities of these particles are listed in Table 2. As noted earlier, the desired fluidization regime for hot sand bed is turbulent (or fast fluidization), while fluidized regime for biomass particles is pneumatic conveying. Kunii and Levenspiel [69] have given a comprehensive charts of fluidization regimes in terms of non–dimensional velocity (u^*) and non–dimensional particle size (d_p^*) for solid particles in different categories (A, B, C and D based on their physical properties). The range of actual gas velocities required for having sand particles in turbulent (fast fluidization) mode and biomass particles in pneumatic conveying mode is given in Table 2. On the basis of above analysis, we decided the superficial air velocity through the riser as 3.5 m/s, which corresponds correspond to volumetric flow rate of 100 Nm^3/h for cross–sectional area of 0.0081 m^2 of the riser. For this air velocity, sand particles will always be in the turbulent or fast fluidization regime, while biomass particles will be in pneumatic conveyance regime.

The pyrolysis products emerging from the turbulent sand bed have different velocities. The larger the diameter of riser, the larger is the spatial velocity distribution in the gasification mixture passing through the riser. However, for small diameter (ID 4 in.) riser as considered in this study, one can assume a uniform velocity profile across the cross–section, without any back–mixing. Thus, the gasification mixture essentially passes in a plug flow manner through the riser.

3- Air ratio and biomass feed rate

Another important factor is the air or equivalence ratio (the ratio of actual moles of air supplied to the stoichiometric moles of air required for complete oxidation of biomass). In a previous study, we have shown that for gasification temperature range of 700 – 1000^{o}C, the optimum range of air ratio is 0.2–0.4. On the basis of this result, we have chosen three air ratios for our analysis, viz. 0.2. 0.3 and 0.4. At the NTP conditions, 100 m^3/h air would correspond to 4089 mol/h or 1.136 mol/s. This would essentially mean O_2 flow rate of 2.3856×10^{-3} kmol/s and N_2 flow rate of 8.9744×10^{-3} kmol/s. The actual air requirement for biomass gasification depends on elemental composition or ultimate analysis of biomass. We have considered rice husk and wood particles (or dust) as biomass in this study and the ultimate

analysis and elemental composition of the same is given in Table 3(a and b), respectively. On the basis of ultimate analysis of biomass, the actual air requirement in moles for 100 g of biomass at different air ratios (0.2, 0.3 and 0.4) is given in Table 3 c. On the basis of this, the biomass feed rate required for achieving these air ratios (corresponding to fixed air flow of 100 Nm^3/h) at the inlet of the gasifier is calculated, and given in Table 3 c.

Table 2. Hydrodynamic properties of sand and biomass particles in the fluidized bed

Property	Sand	Biomass Particles		
d_p (μm)	271	250	500	1000
φ_s (–)	0.8	0.8	0.8	0.8
ρ (kg m^{-3})	2600	120	120	120
u_{mf} (m s^{-1})	0.028	1.08×10^{-3}	4.32×10^{-3}	0.017
$Re_{p,mf}$ (–)	0.254	9.13×10^{-3}	0.073	0.584
d_p^* (–)	7.85	2.59	5.18	10.36
u_t^* (–)	1.69	0.31	0.96	2.34
u_t (m/s)	1.45	0.096	0.29	0.72
u^* (range)[a]	2 – 10	2 – 11	3 – 12	4 – 30
u (range, m s^{-1})	1.71 – 8.56	0.61 – 3.37	0.92 – 3.67	1.23 – 9.18

Properties of fluidizing medium: $\rho_{air} = 1.2$ kg m^{-3}, $\mu_{air} = 3.546 \times 10^{-5}$ Pa-s, $\varepsilon_{mf} = 0.4$.
[a] The range of u^* values is for fast fluidization regime in case of sand particles, and for pneumatic conveying regime for biomass particles.

Table 3. Data on biomasses

(a) Ultimate analysis

Biomass	Composition in weight percent (Dry Basis)				
	Carbon	Hydrogen	Nitrogen	Oxygen	Ash
Wood chips	40.3	5.7	0.3	38.4	15.3
Rice husk	46.4	5.9	0.09	47.17	0.45

(b) Elemental composition and molecular formula for biomasses

Biomass	Composition in gatom (per 100 g biomass)				Molecular Formula
	Carbon (C)	Hydrogen (H)	Nitrogen (N)	Oxygen (O)	
Wood chips	3.36	5.70	0.30	2.40	$CH_{1.696}N_{0.09}O_{0.714}$
Rice husk	3.87	5.90	0.01	2.95	$CH_{1.525}N_{0.002}O_{0.762}$

(c) Air and biomass flow rate in the CFB gasifier

Biomass	Air Ratio (AR)	Air requirement (in gmoles) for 100 g biomass	Biomass Flow Rate[a] (g s^{-1})
Rice Husk	0.2	2.985	38.06
	0.3	4.477	25.37
	0.4	5.969	19.03
Wood Particles	0.2	3.701	30.69
	0.3	5.552	20.46
	0.4	7.402	15.34

[a] This value is calculated on the basis of 100 Nm^3/h of air flow rate to the riser of the gasifier.

5.4 Input for the equilibrium model

Input to the equilibrium model is in the form of an elemental vector, which is determined from the moles of air and the elemental composition of amount of biomass fed to the gasifier (which in turn is determined from the ultimate analysis of biomass). As noted earlier, the moles of air fed to the riser of the gasifier are 1.136 mol/s (or 4089 mol/h corresponding to volumetric flow rate of 100 m^3/h). The biomass feed rate required for having air ratio of 0.2, 0.3 or 0.4 is given in Table 3 c. The elemental vector in the present simulations is calculated using these values. For the equilibrium model, we consider complete conversion of carbon present in the biomass, while for the semi–equilibrium model we put restriction on the extent of carbon conversion. Thus, the g atoms of carbon in the elemental vector input are reduced by $(1 - x_c)$, where x_c is the extent of carbon conversion. The carbon conversion achieved in gasification through a circulating fluidized bed gasifier depends on several parameters. Main among these are: (1) temperature, (2) biomass particle size, (3) air ratio, and (4) residence time of particles in the riser. Some of these factors are inter–dependent, i.e. heat released with conversion of carbon raises the temperature of gasification mixture, which further boosts the kinetics of carbon gasification. However, due to limited residence time of biomass in gasifier, conversion of carbon in biomass in a single pass through riser is not complete, and unconverted carbon appears in the form of char. On the basis of values of carbon conversions in experimental studies using CFB gasifiers (either lab or pilot scale) by [68, 70-72], we have selected two levels of carbon conversion for our simulation with semi–equilibrium model, viz. 60% and 80%. The complete elemental vector for different sets of simulations is depicted in Table 4.

Table 4. Elemental vector input for equilibrium and semi-equilibrium models

Biomass: Rice Husk				**Biomass: Wood Chips**			
Carbon Conversion: 60%				**Carbon Conversion: 60%**			
Element /	AR			Element /	AR		
Elemental Ratio	0.2	0.3	0.4	Elemental Ratio	0.2	0.3	0.4
C	0.767	0.511	0.383	C	0.712	0.475	0.356
H	3.281	2.557	2.196	H	2.922	2.318	2.016
N	2.073	2.070	2.069	N	1.799	1.798	1.797
O	2.015	1.710	1.558	O	1.935	1.633	1.482
H/C	2.567	3.001	3.437	H/C	2.462	2.930	3.400
O/H	0.614	0.669	0.709	O/H	0.662	0.704	0.735
O/C	1.577	2.007	2.438	O/C	1.630	2.064	2.499
Carbon Conversion: 80%				**Carbon Conversion: 80%**			
Element /	AR			Element /	AR		
Elemental Ratio	0.2	0.3	0.4	Elemental Ratio	0.2	0.3	0.4
C	1.022	0.682	0.511	C	0.950	0.633	0.474
H	3.281	2.557	2.196	H	2.922	2.318	2.016
N	2.073	2.070	2.069	N	1.799	1.798	1.797
O	2.015	1.710	1.558	O	1.935	1.633	1.482
H/C	1.063	0.829	0.712	H/C	2.462	2.930	3.400
O/H	0.614	0.669	0.709	O/H	0.662	0.704	0.735
O/C	0.653	0.554	0.505	O/C	1.630	2.064	2.499
Carbon Conversion: 100%				**Carbon Conversion: 100%**			
Element /	AR			Element /	AR		
Elemental Ratio	0.2	0.3	0.4	Elemental Ratio	0.2	0.3	0.4
C	1.278	0.852	0.639	C	1.187	0.791	0.593
H	3.281	2.557	2.196	H	2.922	2.318	2.016
N	2.073	2.070	2.069	N	1.799	1.798	1.797
O	2.015	1.710	1.558	O	1.935	1.633	1.482
H/C	1.063	0.829	0.712	H/C	2.462	2.930	3.400
O/H	0.614	0.669	0.709	O/H	0.662	0.704	0.735
O/C	0.653	0.554	0.505	O/C	1.630	2.064	2.499

5.5 Input for kinetic model

Input to the kinetic model is in terms of the molar flow rates of species forming out of pyrolysis of biomass entering the gasifier. The composition of the pyrolysis products depend on several factors such as biomass particle size, temperature, gasification medium etc. Several authors have studied the product distribution from fast pyrolysis of biomass particles, in which the biomass particles are suddenly expressed to high temperature environment (for example, [17, 73-86]). The product distribution from pyrolysis is mainly a function of temperature. For our study, we take the results of Di Blasi et al. [86] on pyrolysis characteristics of agro–residues as basis.

Di Blasi et al. [86] have studied the pyrolysis of rice husk and wood particles, and have reported the distribution of pyrolysis products, viz. char, tar and gaseous species, viz. CO, CO_2, H_2, CH_4, C_2H_4 and C_2H_6 (on the basis of moisture free biomass) as a function of temperature of pyrolysis. We have reproduced the results of Di Blasi et al. [86] in Figures 1 and 2. We have fitted polynomial expressions to the results of Di Blasi et al. [86]. The best fit expressions for yields of various species are listed in Table 5 (a and b) for rice husk and wood particles, respectively. The actual yield of these species (in either kg/s or kmol/s) at gasification temperature of 973 and 1073 K (700 and 800 ^oC) and air ratios of 0.2, 0.3 and 0.4 is given in Tables 6 and 7 for rice husk and wood particles, respectively. These values form input to the kinetic model.

The extent of carbon conversion for kinetic model is determined by residence time of gasification mixture in the riser section. This factor is determined by the velocity of the gasification mixture and the length of the riser. We have considered two lengths of the riser, viz. 6 m and 10 m above the turbulent sand bed from which the pyrolysis products emerge. This would essentially give reaction volumes of 0.0486 m^3 and 0.081 m^3, respectively.

5.6 Simulation sets

With permutation–combination of 3 air ratios (0.2, 0.3 and 0.4), 2 gasification temperatures (700 and 800^oC), and 3 levels of carbon conversions (viz. 100% for equilibrium model and 60 and 80% for semi–equilibrium model), we get 18 simulation sets with thermodynamic equilibrium and semi–equilibrium models for each biomass, viz. rice husk and wood particles. For the kinetic model, we have essentially 12 simulation sets for each biomass with permutation combination of 3 air ratios, 2 gasification temperatures and two reaction volumes.

Table 5. Pyrolysis correlations

(a) Correlations for yield of various components resulting from rice husk pyrolysis

Sr. No.	Component	Correlation
1.	Char	$y_{char} = 1.055\times10^{-4}T^2 - 0.22016T + 150.4764$
2.	Tar	$y_{tar} = 1.582\times10^{-4}T^2 + 0.28218T - 92.1972$
3.	Gas (total)	$y_{gas} = 1.154\times10^{-4}T^2 - 0.15576T + 67.5489$
	Individual gas Components	
4.	CO	$y_{CO} = 7.261\times10^{-5}T^2 - 0.10416T + 42.0829$
5.	CO_2	$y_{CO_2} = 2.534\times10^{-5}T^2 - 0.03036T + 18.7576$
6.	H_2	$y_{H_2} = 6.198\times10^{-6}T^2 - 9.6545T + 3.75195$
7.	CH_4	$y_{CH_4} = 7.954\times10^{-6}T^2 - 6.9416\times10^{-3}T + 1.2026$
8.	C_2H_4+C_2H_6	$y_{C_2H_4+C_2H_6} = 3.568\times10^{-6}T^2 - 3.8788\times10^{-3}T + 1.01864$

(b) Correlations for yield of various components resulting from wood particles pyrolysis

Sr. No.	Component	Correlation
1.	Char	$y_{char} = -5.694\times10^{-9}T^2 + 1.897\times10^{-5}T^3 - 0.0233T^2 + 12.4438T - 2395.73$
2.	Tar	$y_{tar} = -1.114\times10^{-8}T^4 + 3.787\times10^{-5}T^3 - 0.04821T^2 + 27.247T - 5719.65$
3.	Gas (total)	$y_{gas} = 1.793\times10^{-9}T^4 - 6.198\times10^{-6}T^3 + 8.039\times10^{-3}T^2 - 4.5927T + 988.76$
	Individual gas Components	
4.	CO	$y_{CO} = 6.675\times10^{-10}T^4 - 2.437\times10^{-6}T^3 + 3.369\times10^{-3}T^2 - 2.05453T + 468.25$
5.	CO_2	$y_{CO_2} = 1.342\times10^{-9}T^4 - 4.414\times10^{-6}T^3 + 5.373\times10^{-3}T^2 - 2.8624T + 574.28$
6.	H_2	$y_{H_2} = 1.852\times10^{-10}T^4 - 5.478\times10^{-7}T^3 + 7.221\times10^{-4}T^2 - 0.38626T + 77.131$
7.	CH_4	$y_{CH_4} = 2.338\times10^{-10}T^4 - 8.289\times10^{-7}T^3 + 1.1029\times10^{-3}T^2 - 0.64438T + 139.2$
8.	C_2H_4+C_2H_6	$y_{C_2H_4+C_2H_6} = -1.133\times10^{-10}T^4 + 3.625\times10^{-7}T^3 - 4.25\times10^{-4}T^2 + 0.21849T - 41.686$

Table 6. Distribution of products of pyrolysis of rice husk at different temperatures and air ratio

(a) Temperature 700 ºC

Component	AR = 0.2		AR = 0.3		AR = 0.4	
	Yield (kmol/s)	Concentration (kmol/m^3)	Yield (kmol/s)	Concentration (kmol/m^3)	Yield (kmol/s)	Concentration (kmol/m^3)
Char (kg/s)	1.373E–02	–	9.179E–03	–	6.866E–03	–
Tar	7.741E–04	0.15663	5.174E–04	0.10469	1.704E–04	0.03447
CO	1.286E–04	0.02602	8.596E–05	0.01739	6.43E–05	0.01301
CO_2	1.141E–04	0.02308	7.624E–05	0.01543	5.703E–05	0.01154
H_2	4.293E–05	0.00869	2.87E–05	0.00581	2.147E–05	0.00434
CH_4	4.7E–05	0.00951	3.141E–05	0.00636	2.35E–05	0.00475
C_2H_4	4.224E–06	0.00085	2.823E–06	0.00057	2.112E–06	0.00043
C_2H_6	3.942E–06	0.0008	2.635E–06	0.00053	1.971E–06	0.0004
H_2O	2.111E–04	0.04272	1.411E–04	0.02855	1.056E–04	0.02136

(b) Temperature 800 ºC

Component	AR = 0.2		AR = 0.3		AR = 0.4	
	Yield (kmol/s)	Concentration (kmol/m^3)	Yield (kmol/s)	Concentration (kmol/m^3)	Yield (kmol/s)	Concentration (kmol/m^3)
Char (kg/s)	1.357E–02	–	8.927E–03	–	6.784E–03	–
Tar	6.755E–04	0.13669	4.444E–04	0.08993	3.378E–04	0.06834
CO	1.889E–04	0.03821	1.242E–04	0.02514	9.443E–05	0.01911
CO_2	1.326E–04	0.02683	8.725E–05	0.01765	6.631E–05	0.01342
H_2	1.004E–04	0.02032	6.608E–05	0.01337	5.022E–05	0.01016
CH_4	6.916E–04	0.01399	4.550E–05	0.00921	3.458E–05	0.00700
C_2H_4	6.546E–06	0.00132	4.306E–06	0.00087	3.273E–06	0.00066
C_2H_6	6.109E–06	0.00124	4.019E–06	0.00081	3.055E–06	0.00062
H_2O	2.111E–04	0.04272	1.389E–04	0.02810	1.056E–04	0.02136

Table 7. Distribution of products of pyrolysis of wood particles at different temperatures and air ratios

(a) Temperature 700 ºC

Component	AR = 0.2		AR = 0.3		AR = 0.4	
	Yield (kmol/s)	Concentration (kmol/m^3)	Yield (kmol/s)	Concentration (kmol/m^3)	Yield (kmol/s)	Concentration (kmol/m^3)
Char (kg/s)	6.964E–03	–	4.718E–03	–	3.594E–03	–
Tar	9.474E–04	0.1917	6.418E–04	0.12986	4.89E–04	0.09894
CO	1.351E–04	0.02734	9.154E–05	0.01852	6.974E–05	0.01411
CO_2	8.981E–05	0.01817	6.084E–05	0.01231	4.636E–05	0.00938
H_2	3.92E–05	0.00793	2.655E–05	0.00537	2.023E–05	0.00409
CH_4	4.591E–05	0.00929	3.11E–05	0.00629	2.369E–05	0.00479
C_2H_4	5.07E–06	0.00103	3.435E–06	0.00069	2.617E–06	0.00053
C_2H_6	4.732E–06	0.00096	3.206E–06	0.00065	2.442E–06	0.00049
H_2O	1.722E–04	0.03485	1.167E–04	0.02361	8.889E–05	0.01799

(b) Temperature 800 ºC

Component	AR = 0.2		AR = 0.3		AR = 0.4	
	Yield (kmol/s)	Concentration (kmol/m^3)	Yield (kmol/s)	Concentration (kmol/m^3)	Yield (kmol/s)	Concentration (kmol/m^3)
Char (kg/s)	4.781E–03	–	3.177E–03	–	2.336E–03	–
Tar	5.132E–04	0.10384	3.410E–04	0.06900	2.507E–04	0.05074
CO	1.850E–04	0.03744	1.230E–04	0.02488	9.041E–05	0.01829
CO_2	1.045E–04	0.02114	6.944E–05	0.01405	5.106E–05	0.01033
H_2	1.587E–04	0.03212	1.055E–04	0.02134	7.755E–05	0.01569
CH_4	6.714E–05	0.01358	4.461E–05	0.00903	3.280E–05	0.00664
C_2H_4	5.893E–06	0.00119	3.916E–06	0.00079	2.879E–06	0.00058
C_2H_6	5.500E–06	0.00111	3.655E–06	0.00074	2.687E–06	0.00054
H_2O	1.706E–04	0.03451	1.133E–04	0.02293	8.333E–05	0.01686

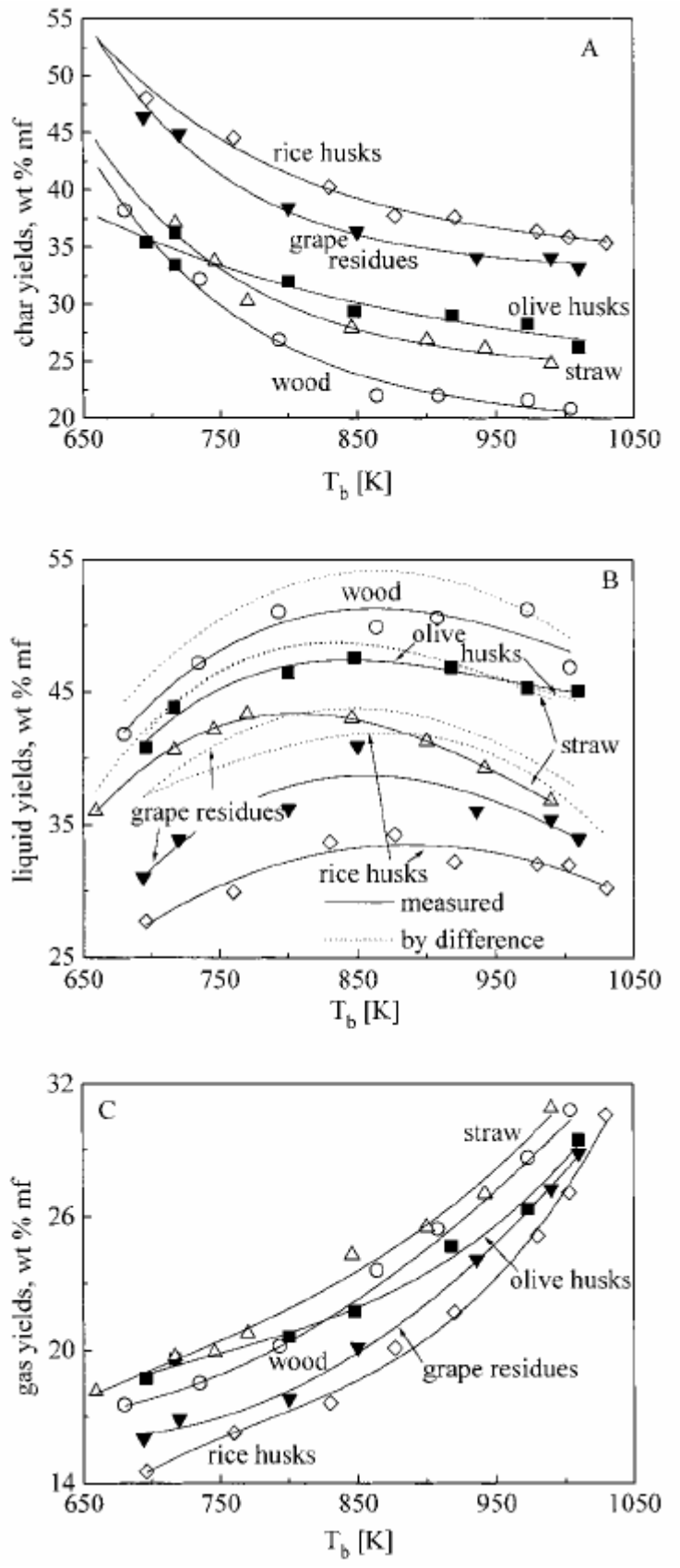

Figure 1. Yield of different pyrolysis products (as wt% of moisture free biomass): (A) char, (B) liquid or tar, and (C) gas from various biomass, as a function of temperature of pyrolysis (reproduced from Di Blasi et al., [86] with permission of American Chemical Society)

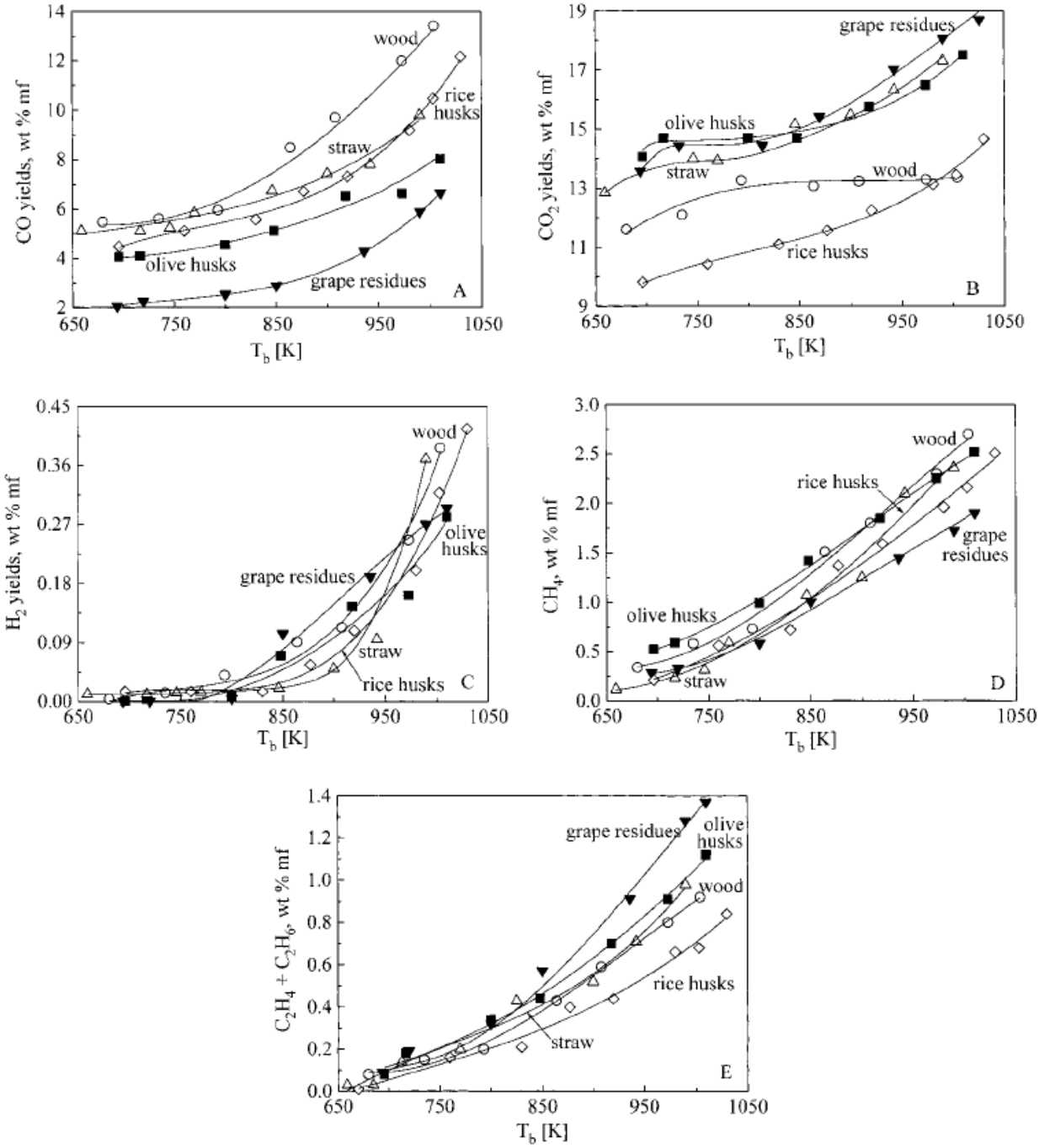

Figure 2. Yield of different gas species from pyrolysis of various biomass (as wt% of moisture free biomass): (A) CO, (B) CO_2, (C) H_2, (D) CH_4, (E) $C_2H_4 + C_2H_6$, as a function of temperature of pyrolysis (reproduced from Di Blasi et al., [86] with permission of American Chemical Society)

6. Results and discussion

We have presented the results of simulations in three parts. We begin with presentation of the results with kinetic model, followed by results with equilibrium and semi–equilibrium models. Finally, we present a comparative analysis of the results with all three models. The simulation results for all three models comprise of: (1) the molar composition of the gas, (2) net yield (Nm^3) of the gas, and (3) the LHV (MJ/Nm^3) of the gas. In case of kinetic model, we have also presented the profiles of char formation and char gasification /combustion under different sets of operating conditions. Figures 3 and 4 depict the molar composition of producer gas calculated for rice husk using kinetic model for different air ratios at 700 and 800^oC respectively, while Figures 5 and 6 present the molar composition of producer gas for wood particles gasification at 700 and 800^oC. Figure 7 shows the trends in formation of char (as

wt% of initial moisture free biomass) for rice husk and wood particles, while Figure 8 shows the extent of gasification of char (wt% of initial char) in the riser at different gasification of char (wt% of initial char) in the riser at different air ratios and temperature. Figures 9 and 10 show molar composition of producer gas resulting from gasification of rice husk at 700^{o}C and 800^{o}C using equilibrium and semi–equilibrium models. Figures 11 and 12 depict the molar composition of producer gas for wood particle gasification calculated using equilibrium and semi–equilibrium models at 700^{o}C and 800^{o}C respectively. Figures 13 and 14 describe the trends in net producer gas yield and LHV of the producer gas resulting from gasification of wood particles and rice husk, respectively, calculated using kinetic model under different gasifying conditions. Figures 15 and 16 show the trends of producer gas yield and LHV of the gas for wood particles and rice husk gasification under different conditions calculated using equilibrium and semi–equilibrium models. For convenience of the readers, we have also added data tables in Figures 3-5 and 9-16. In our analysis, we initially identify the (qualitative) trends in the molar of gas, producer gas yield, LHV of the gas and the composition of gas and char formation/gasification (in case of kinetic model only) for the two models. Subsequently, we attempt to do quantitative comparison of the simulation results with various models.

6.1 Analysis of results of kinetic model

1- Trends in molar composition of producer gas

The composition of products resulting from pyrolysis of biomass emanating from the hot sand bed (or the pyrolysis zone) is given in Tables 6 and 7 for different operating conditions. Fraction of two key components of the producer gas, viz. CO and H_2 generated in pyrolysis shows drastic reduction with increasing air ratio. However, the fraction of these gases shows marginal increase with temperature of pyrolysis. As the gasification mixture emerges out of pyrolysis zone and travels upward in the riser, an interesting observation is seen for carbon monoxide in that it shows a maxima with volume of riser. Fraction of CO in the producer gas for riser of 10 m height is less than that for 6 m height. As in pyrolysis, the fraction of CO and H_2 in the final producer gas resulting from gasifier also shows reduction with air ratio, and marginal rise with temperature. Extent of CO_2 generation in pyrolysis is rather insensitive to temperature. As the gasification proceeds the fraction of CO_2 in the producer gas increases. The extent of this rise, obviously, varies directly with the air ratio and inversely with the temperature of gasification. Volume of the riser, however, has no effect on the fraction of CO_2 in the producer gas. Tar content of the gas generated from pyrolysis shows reduction with temperature. Thereafter, however, the reduction in tar content is rather low, due to slow kinetics of tar oxidation. The tar content of the gas (in terms of moles) remains almost constant from pyrolysis zone till exit from the gasifier. Composition of methane, ethane and ethylene in the gas is quite small, and shows marginal reduction from pyrolysis zone till exit from gasifier. In the pyrolysis zone, the extent of generation of these three gases shows increase with temperature. Once again, the volume of the gasifier has no effect on the composition of these species in the final gas. Char generation and subsequent gasification also shows interesting trends. As seen from Figure 7, a significant mass fraction of biomass ends up in the form of char. This fraction (with respect to moisture free biomass) is practically independent of the air ratio. However, it shows reduction with temperature of pyrolysis. Comparing among the two biomass used in this study, we see that reduction in weight fraction of char is more marked for wood particles than rice husk. Some interesting trends in the gasification (or oxidation) of the char are seen in Figure 8. These are (1) extent of char gasification increases with air ratio, (2) fractional gasification of char reduces with temperature (for a particular air ratio and gasification volume), and (3) fractional gasification of char is independent of the volume of the gasifier.

2- Trends in net gas yield and LHV

The yield of producer gas shows small reduction with increasing air ratio (for given gasifier volume and temperature), marginal rise with temperature of gasification (for a given air ratio and gasification volume) and rather insensitivity to volume of gasifier. The LHV of the producer gas shows following trends: (1) rise with gasification temperature for given air ratio and reactor volume, (2) reduction with air ratio for a given gasification temperature and reactor volume, and (3) reduction with increasing reactor volume for a given air ratio and gasification temperature. Comparing among the two biomasses, we observe that fluctuations in LHV are more marked for wood chops than rice husk. In fact, for air ratios of 0.3 and 0.4, the LHV of producer gas from rice husk becomes almost independent of gasification temperature and reactor volume. For air ratio 0.2 and temperature 800^{o}C (1073 K), the LHV of producer

gas shows a drastic 10 fold rise, as compared to the LHV at 700°C at same air ratio. This trend demonstrates critical sensitivity of LHV towards gasification temperature at low air ratios.

6.2 Analysis of equilibrium and semi–equilibrium model

1- Trends in molar composition

From the results presented in Figures 7-10, we can identify following trends in the content of the producer gas with operating parameters: (1) Fraction of both H_2 and CO shows inverse variation with air ratio. However , CO content of gas shows direct variation with temperature of gasification, while H_2 content reduces with increasing temperature for a particular air ratio and level of carbon conversion.(2) Obviously, the number of moles of both H_2 and CO reduce with extent of carbon conversion. (3) Amount of CO_2 in the producer gas shows relative insensitivity towards air ratio for high carbon conversion. However, for low carbon conversion (60%), the CO_2 content of producer gas shows significant reduction with air ratio. (4) Amount of H_2O in the producer gas shows increase with both air ratio and temperature of gasification. (5) Methane content of the gas is quite small, and for high air ratio of 0.4, methane content practically reduces to zero, (6) No formation of any other hydrocarbon such as ethane, ethylene or even higher hydrocarbon is seen under equilibrium conditions (i.e. 100% carbon conversion). However, for the semi–equilibrium conditions, the unconverted carbon can appear in the form of char, tar and other hydrocarbons, (7) Comparing among the two biomass, slightly lesser CO and H_2 is seen in the producer gas resulting from gasification of wood particles than rice husk under similar operating conditions. Amount of CO_2 in the producer gas, however, is higher for wood particles than rice husk.

2- Trends in LHV and gas yield

(1) For a given air ratio and gasification temperature, the gas yield obviously reduces with carbon conversion, (2) Gas yield reduces with increasing air ratio at a given gasification temperature and level of carbon conversion, (3) Temperature, however, is not a significant parameter affecting gas yield. At any air ratio and level of carbon conversion, the net gas yield at both 700 and 800°C is essentially the same. (4) Comparing among rice husk and wood particles, we find higher gas yield for wood particles, and this is obviously attributed to higher ash content of rice husk. Trends in LHV are as follows: (1) For a given gasification temperature and air ratio, the LHV of the producer gas obviously falls with carbon conversion, (2) LHV also shows inverse trend with air ratio for a particular gasification temperature and carbon conversion, (3) Like the net gas yield, temperature does not seem to influence the LHV significantly for same gasification temperature and air ratio, (4) Higher LHV of producer gas is seen for wood particles than rice husk under similar gasifying conditions. This is attributed to higher carbon content of wood particles that results in higher CO content of the producer gas.

6.3 Comparative analysis of three models

The trends in the net yield and characteristics of the producer gas resulting from gasification of wood particles and rice husk predicted by the three models are in concurrence. Nonetheless, the results of simulations (molar composition of gas, net gas yield and LHV of producer gas) from the three models show significant quantitative difference. The quantitative comparison of the results of three models clearly indicates that the gasification mixture is far from equilibrium (even with as height of riser as 10 m), and the overall carbon conversion in single pass is very small (~ 30–40%). Major differences are: (1) extent carbon monoxide and hydrogen content of the producer gas as predicted by kinetic model is much smaller than that calculated using equilibrium and semi–equilibrium models. Equilibrium and semi–equilibrium models do not predict formation of any other hydrocarbon than CH_4, while kinetic model gives smaller quantities of ethane and ethylene. Significant fraction of carbon in the biomass remains unconverted in the form char. The tar produced in the pyrolysis zone also remains unconverted (or un-oxidized). Thus, both LHV and net gas yield predicted by kinetic model are lesser than equilibrium and semi–equilibrium model, even with least carbon conversion of 60%.

The results of equilibrium and semi–equilibrium model indicate that air ratio is more critical factor influencing biomass conversion to producer gas than temperature. This conclusion is endorsed by kinetic model as well. However, results of kinetic model show that at low air ratios, temperature could have significant influence on net gas yield as well as LHV of the gas. This is evident from results depicted in Figures 13 and 14, where we see sharp rise in gas yield and LHV with temperature rising from 700°C to 800°C. Increasing air ratio at a particular temperature helps enhancement of char gasification; however, it also enhances conversion of H_2 and CO to H_2O and CO_2, respectively, reducing the quality of the

producer gas. Increasing temperature of gasification has adverse effect on char gasification as revealed by Figure 8. This is attributed to factor consumption of O_2 in other parallel reactions in the gasification. Nonetheless, higher temperature prevents conversion of CO and CO_2 and increases the LHV of gas.
The kinetic model also reveals the role of volume of the gasifier (i.e. the height of the riser section of the CFB gasifier) in the gasification process. Relative insensitivity of the gas yield and LHV to the volume of gasifier indicates need for optimization of this parameter. Merely raising the height of the riser section does not help increasing the quality of the gas. This is clearly attributed to slow kinetics of char gasification and tar oxidation. On the other hand, maintenance of proper air ratio and temperature is critical to achieving efficient conversion of biomass to producer gas. The results of the simulation give important clues for enhancing performance of the gasifier. Efficient capture and recycle of the char is crucial to increasing overall carbon conversion in the process. Enhancing oxidation of tar by using a suitable catalyst (sintered–olivine or calcined dolomite) can also augment the gas yield and LHV of the gas. The most critical factor, however, seems to be the pyrolysis of biomass occurring at the bottom of the riser itself. Since the kinetics of char gasification and tar oxidation is rather slow, in that similar extent of char and tar oxidation is achieved at 700 and 800^{o}C, it is imperative to reduce the char and tar formation itself, at the pyrolysis zone. This would mean maintaining significantly higher temperature (~ 1000^{o}C or so) in the pyrolysis zone near the distributor of the riser (i.e. the hot sand bed where biomass entering the gasifier mixes with sand). The temperature in riser section above the pyrolysis zone till gas exit does not make a significant difference, whether 700 or 800^{o}C. An optimization of the pyrolysis in terms of temperature, biomass particle size and use of suitable catalyst, so as to reduce the formation of char and tar, with concurrent enhancement in view of gaseous species, will help increase conversion of biomass to desired species of CO, H_2 and CH_4.

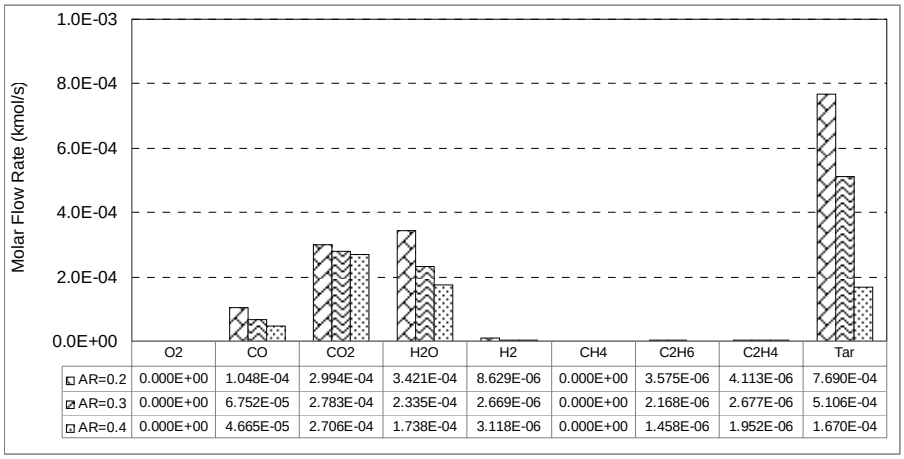

	O2	CO	CO2	H2O	H2	CH4	C2H6	C2H4	Tar
AR=0.2	0.000E+00	1.048E-04	2.994E-04	3.421E-04	8.629E-06	0.000E+00	3.575E-06	4.113E-06	7.690E-04
AR=0.3	0.000E+00	6.752E-05	2.783E-04	2.335E-04	2.669E-06	0.000E+00	2.168E-06	2.677E-06	5.106E-04
AR=0.4	0.000E+00	4.665E-05	2.706E-04	1.738E-04	3.118E-06	0.000E+00	1.458E-06	1.952E-06	1.670E-04

(a)

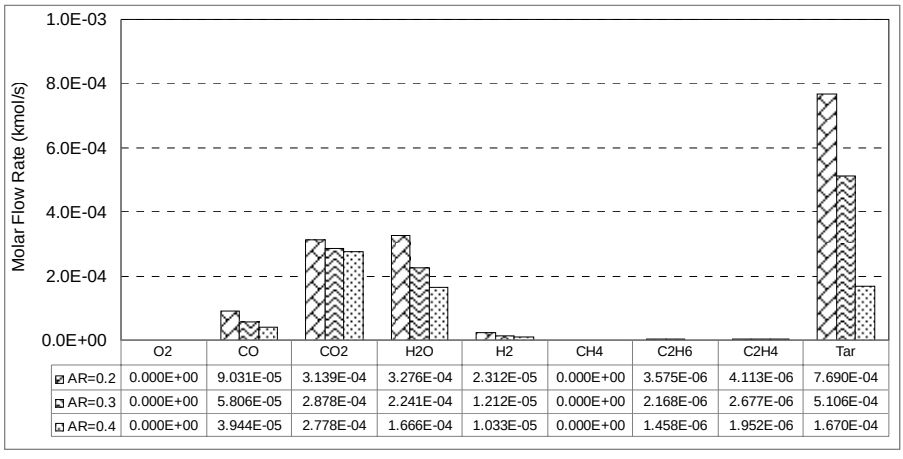

	O2	CO	CO2	H2O	H2	CH4	C2H6	C2H4	Tar
AR=0.2	0.000E+00	9.031E-05	3.139E-04	3.276E-04	2.312E-05	0.000E+00	3.575E-06	4.113E-06	7.690E-04
AR=0.3	0.000E+00	5.806E-05	2.878E-04	2.241E-04	1.212E-05	0.000E+00	2.168E-06	2.677E-06	5.106E-04
AR=0.4	0.000E+00	3.944E-05	2.778E-04	1.666E-04	1.033E-05	0.000E+00	1.458E-06	1.952E-06	1.670E-04

(b)

Figure 3. Results of simulations with kinetic model for rice husk for different gasifying conditions (a) Temperature = 973 K, Volume = 0.0486 m^3; (b) Temperature = 973 K, Volume = 0.08105 m^3

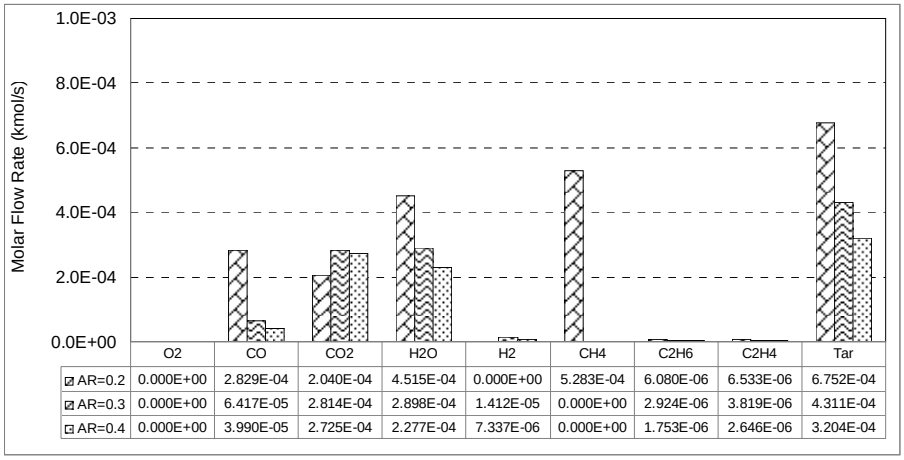

	O2	CO	CO2	H2O	H2	CH4	C2H6	C2H4	Tar
AR=0.2	0.000E+00	2.829E-04	2.040E-04	4.515E-04	0.000E+00	5.283E-04	6.080E-06	6.533E-06	6.752E-04
AR=0.3	0.000E+00	6.417E-05	2.814E-04	2.898E-04	1.412E-05	0.000E+00	2.924E-06	3.819E-06	4.311E-04
AR=0.4	0.000E+00	3.990E-05	2.725E-04	2.277E-04	7.337E-06	0.000E+00	1.753E-06	2.646E-06	3.204E-04

(a)

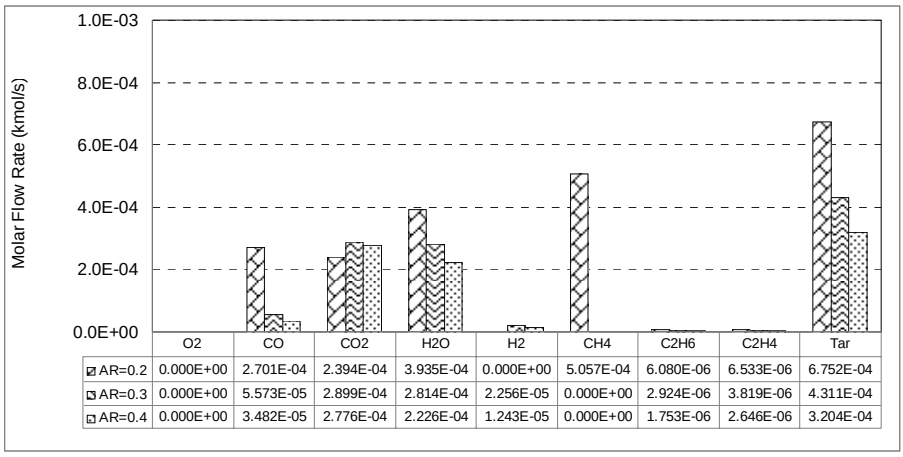

	O2	CO	CO2	H2O	H2	CH4	C2H6	C2H4	Tar
AR=0.2	0.000E+00	2.701E-04	2.394E-04	3.935E-04	0.000E+00	5.057E-04	6.080E-06	6.533E-06	6.752E-04
AR=0.3	0.000E+00	5.573E-05	2.899E-04	2.814E-04	2.256E-05	0.000E+00	2.924E-06	3.819E-06	4.311E-04
AR=0.4	0.000E+00	3.482E-05	2.776E-04	2.226E-04	1.243E-05	0.000E+00	1.753E-06	2.646E-06	3.204E-04

(b)

Figure 4. Results of simulations with kinetic model for rice husk for different gasifying conditions (a) Temperature = 1073 K, Volume = 0.0486 m^3; (b) Temperature = 1073 K, Volume = 0.08105 m^3

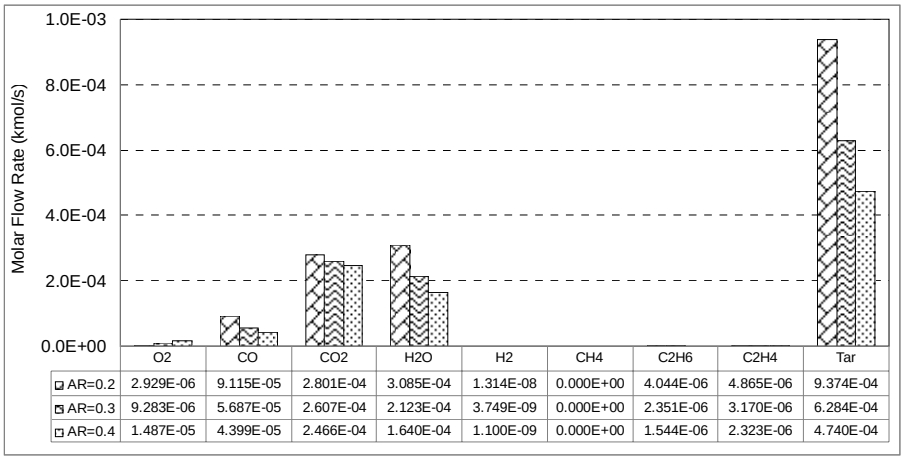

	O2	CO	CO2	H2O	H2	CH4	C2H6	C2H4	Tar
AR=0.2	2.929E-06	9.115E-05	2.801E-04	3.085E-04	1.314E-08	0.000E+00	4.044E-06	4.865E-06	9.374E-04
AR=0.3	9.283E-06	5.687E-05	2.607E-04	2.123E-04	3.749E-09	0.000E+00	2.351E-06	3.170E-06	6.284E-04
AR=0.4	1.487E-05	4.399E-05	2.466E-04	1.640E-04	1.100E-09	0.000E+00	1.544E-06	2.323E-06	4.740E-04

(a)

Figure 5. (Continued)

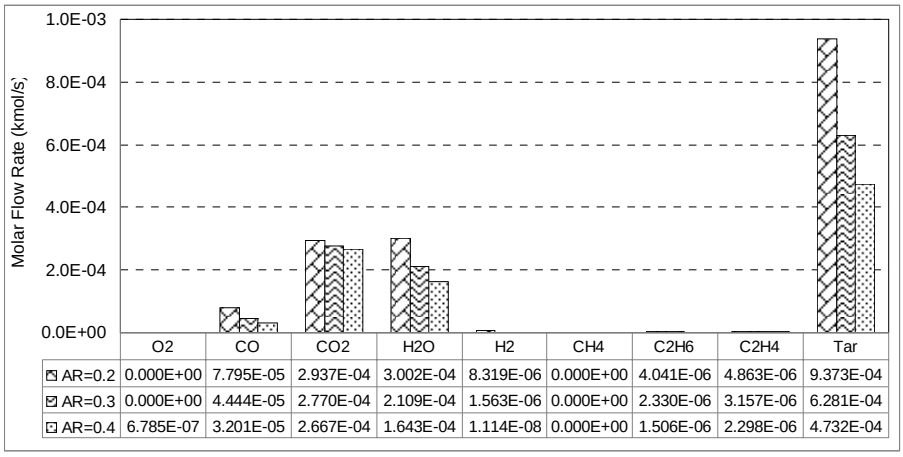

	O2	CO	CO2	H2O	H2	CH4	C2H6	C2H4	Tar
AR=0.2	0.000E+00	7.795E-05	2.937E-04	3.002E-04	8.319E-06	0.000E+00	4.041E-06	4.863E-06	9.373E-04
AR=0.3	0.000E+00	4.444E-05	2.770E-04	2.109E-04	1.563E-06	0.000E+00	2.330E-06	3.157E-06	6.281E-04
AR=0.4	6.785E-07	3.201E-05	2.667E-04	1.643E-04	1.114E-08	0.000E+00	1.506E-06	2.298E-06	4.732E-04

(b)

Figure 5. Results of simulations with kinetic model for wood particles for different gasifying conditions (a) Temperature = 973 K, Volume = 0.0486 m^3; (b) Temperature = 973 K, Volume = 0.08105 m^3

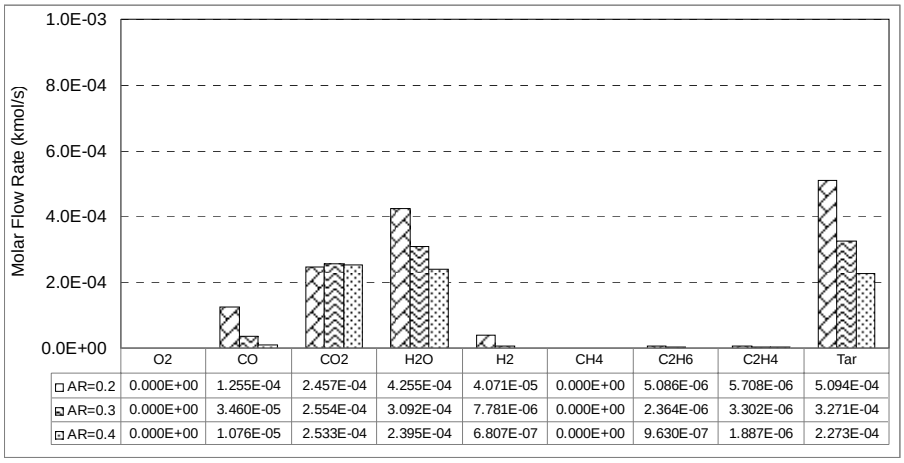

	O2	CO	CO2	H2O	H2	CH4	C2H6	C2H4	Tar
AR=0.2	0.000E+00	1.255E-04	2.457E-04	4.255E-04	4.071E-05	0.000E+00	5.086E-06	5.708E-06	5.094E-04
AR=0.3	0.000E+00	3.460E-05	2.554E-04	3.092E-04	7.781E-06	0.000E+00	2.364E-06	3.302E-06	3.271E-04
AR=0.4	0.000E+00	1.076E-05	2.533E-04	2.395E-04	6.807E-07	0.000E+00	9.630E-07	1.887E-06	2.273E-04

(a)

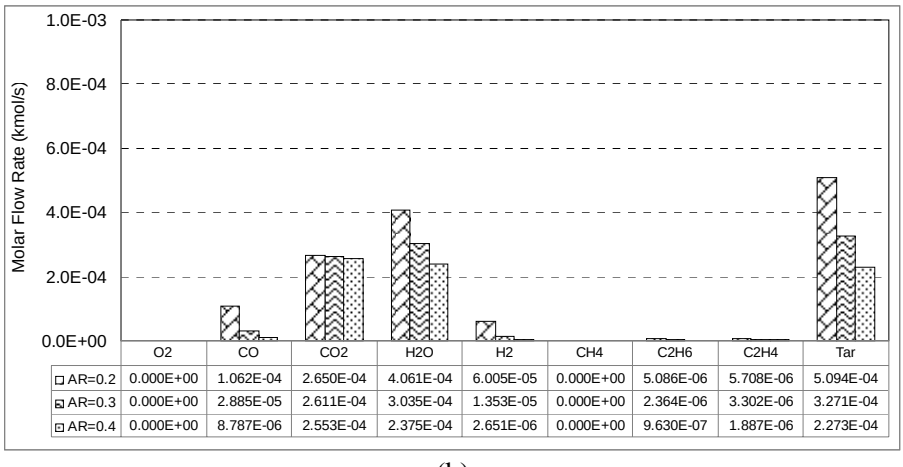

	O2	CO	CO2	H2O	H2	CH4	C2H6	C2H4	Tar
AR=0.2	0.000E+00	1.062E-04	2.650E-04	4.061E-04	6.005E-05	0.000E+00	5.086E-06	5.708E-06	5.094E-04
AR=0.3	0.000E+00	2.885E-05	2.611E-04	3.035E-04	1.353E-05	0.000E+00	2.364E-06	3.302E-06	3.271E-04
AR=0.4	0.000E+00	8.787E-06	2.553E-04	2.375E-04	2.651E-06	0.000E+00	9.630E-07	1.887E-06	2.273E-04

(b)

Figure 6. Results of simulations with kinetic model for wood particles for different gasifying conditions (a) Temperature = 1073 K, Volume = 0.0486 m^3; (b) Temperature = 1073 K, Volume = 0.08105 m^3

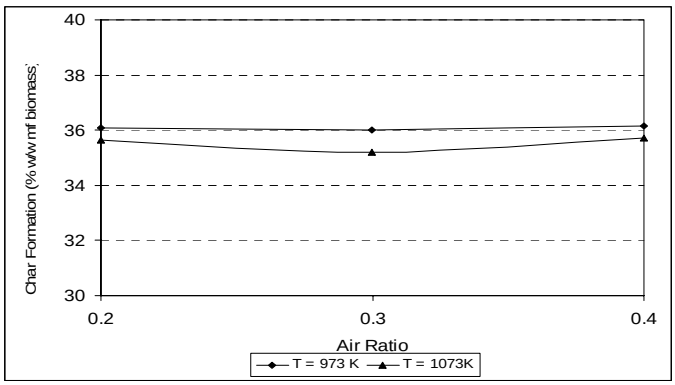

(a)

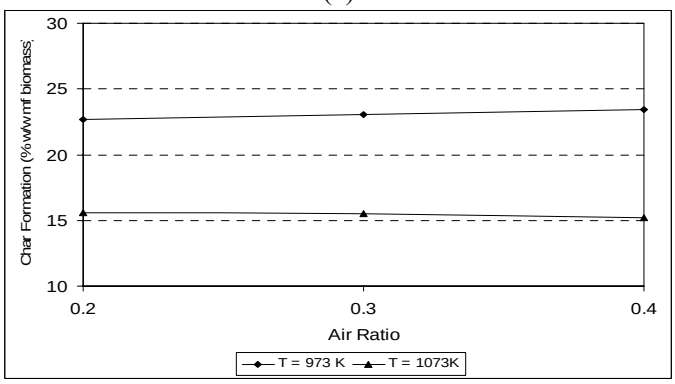

(b)

Figure 7. Trends in char formation (as wt % of initial moisture free biomass0 in the pyrolysis zone at the entry of the gasifier (a) Biomass: Rice husk; (b) Biomass: Wood particles

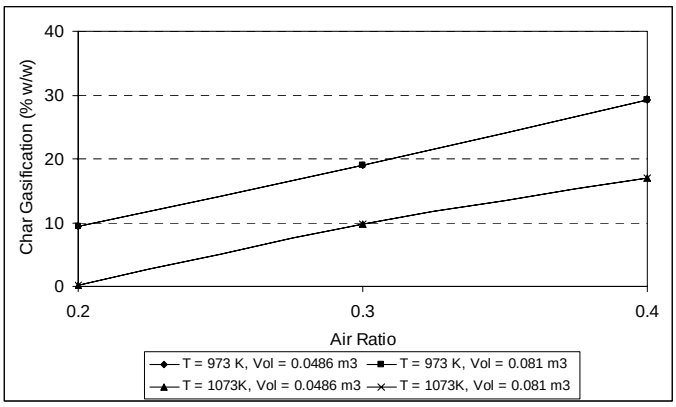

(a)

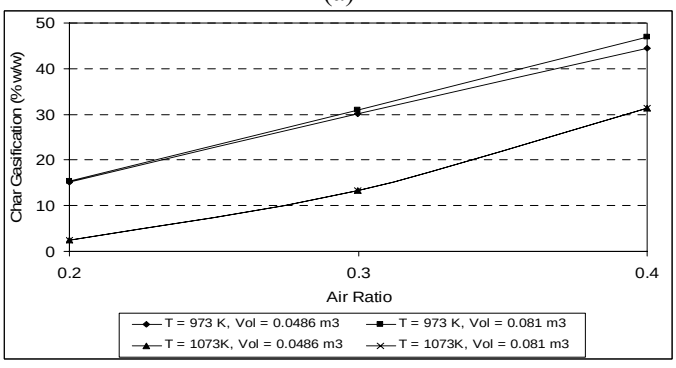

(b)

Figure 8. Results of char gasification (wt % of initial char gasified) in the riser section above pyrolysis (a) Biomass: Rice husk, (b) Biomass: Wood particles

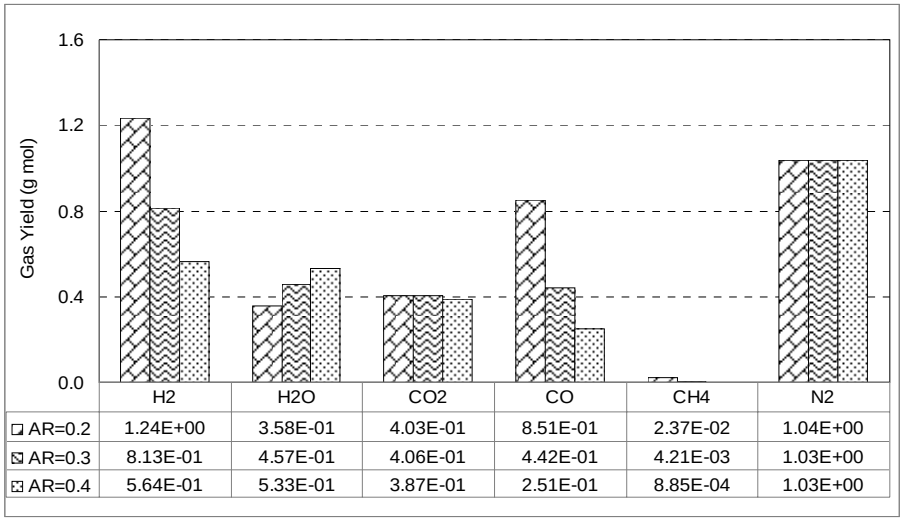

	H2	H2O	CO2	CO	CH4	N2
AR=0.2	1.24E+00	3.58E-01	4.03E-01	8.51E-01	2.37E-02	1.04E+00
AR=0.3	8.13E-01	4.57E-01	4.06E-01	4.42E-01	4.21E-03	1.03E+00
AR=0.4	5.64E-01	5.33E-01	3.87E-01	2.51E-01	8.85E-04	1.03E+00

(a)

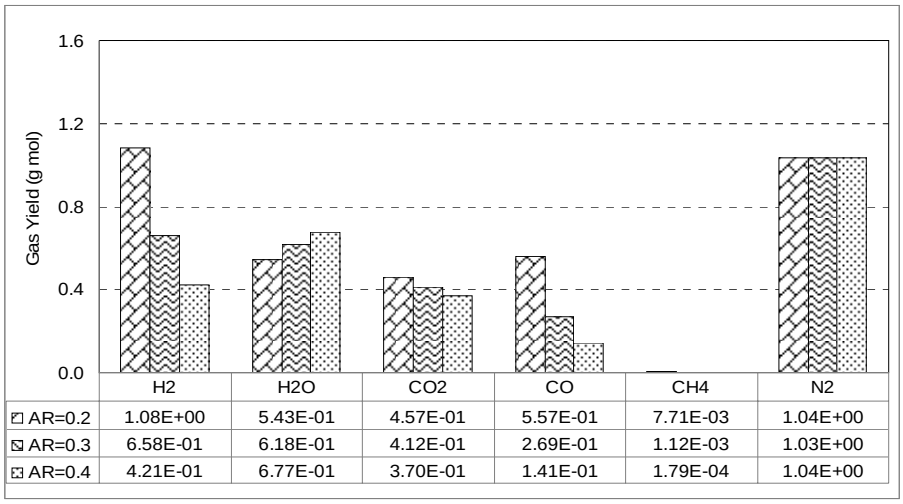

	H2	H2O	CO2	CO	CH4	N2
AR=0.2	1.08E+00	5.43E-01	4.57E-01	5.57E-01	7.71E-03	1.04E+00
AR=0.3	6.58E-01	6.18E-01	4.12E-01	2.69E-01	1.12E-03	1.03E+00
AR=0.4	4.21E-01	6.77E-01	3.70E-01	1.41E-01	1.79E-04	1.04E+00

(b)

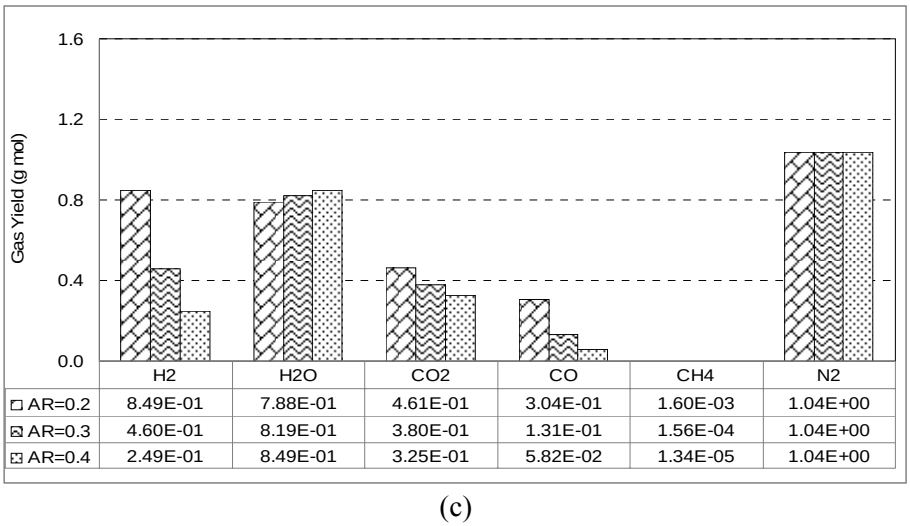

	H2	H2O	CO2	CO	CH4	N2
AR=0.2	8.49E-01	7.88E-01	4.61E-01	3.04E-01	1.60E-03	1.04E+00
AR=0.3	4.60E-01	8.19E-01	3.80E-01	1.31E-01	1.56E-04	1.04E+00
AR=0.4	2.49E-01	8.49E-01	3.25E-01	5.82E-02	1.34E-05	1.04E+00

(c)

Figure 9. Results of simulations of biomass gasification with equilibrium and semi-equilibrium models for rice husk under different gasifying conditions (a) Temperature =973 K, Carbon conversion =100%; (b) Temperature =973 K, Carbon conversion = 80%; (c) Temperature = 973 K, Carbon conversion =60%

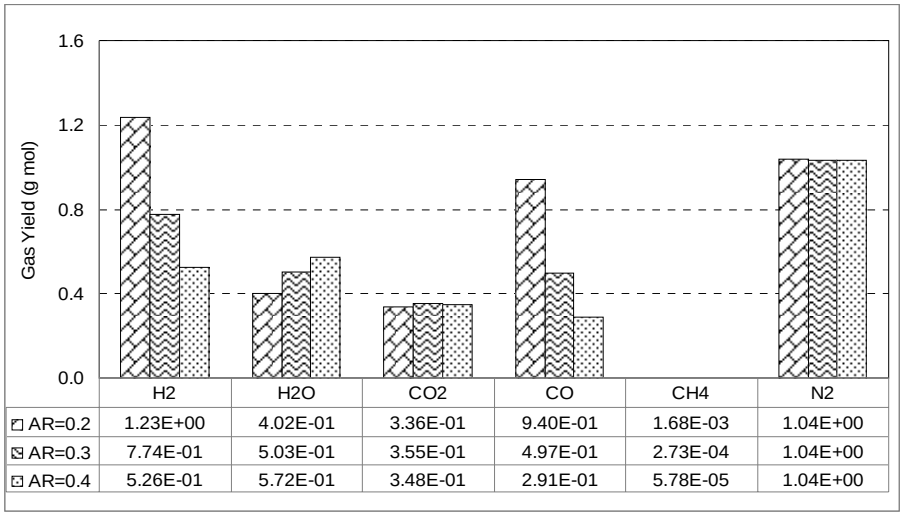

	H2	H2O	CO2	CO	CH4	N2
AR=0.2	1.23E+00	4.02E-01	3.36E-01	9.40E-01	1.68E-03	1.04E+00
AR=0.3	7.74E-01	5.03E-01	3.55E-01	4.97E-01	2.73E-04	1.04E+00
AR=0.4	5.26E-01	5.72E-01	3.48E-01	2.91E-01	5.78E-05	1.04E+00

(a)

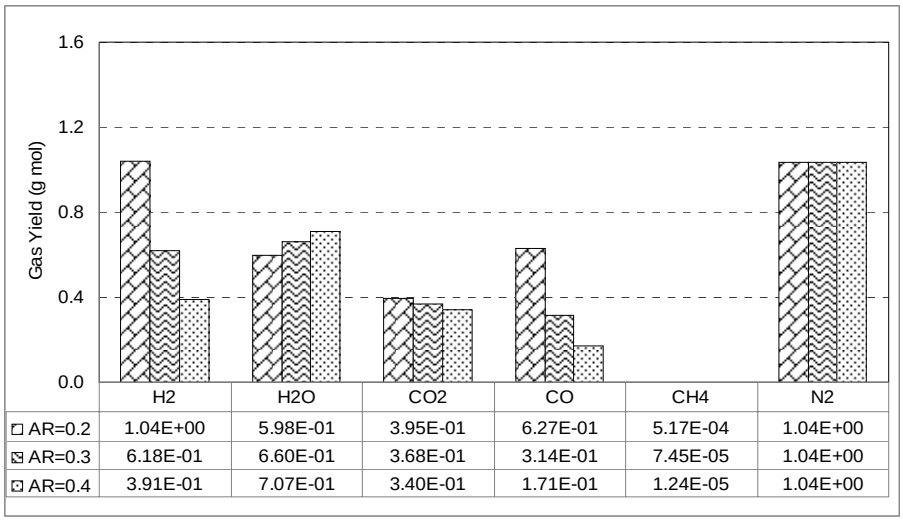

	H2	H2O	CO2	CO	CH4	N2
AR=0.2	1.04E+00	5.98E-01	3.95E-01	6.27E-01	5.17E-04	1.04E+00
AR=0.3	6.18E-01	6.60E-01	3.68E-01	3.14E-01	7.45E-05	1.04E+00
AR=0.4	3.91E-01	7.07E-01	3.40E-01	1.71E-01	1.24E-05	1.04E+00

(b)

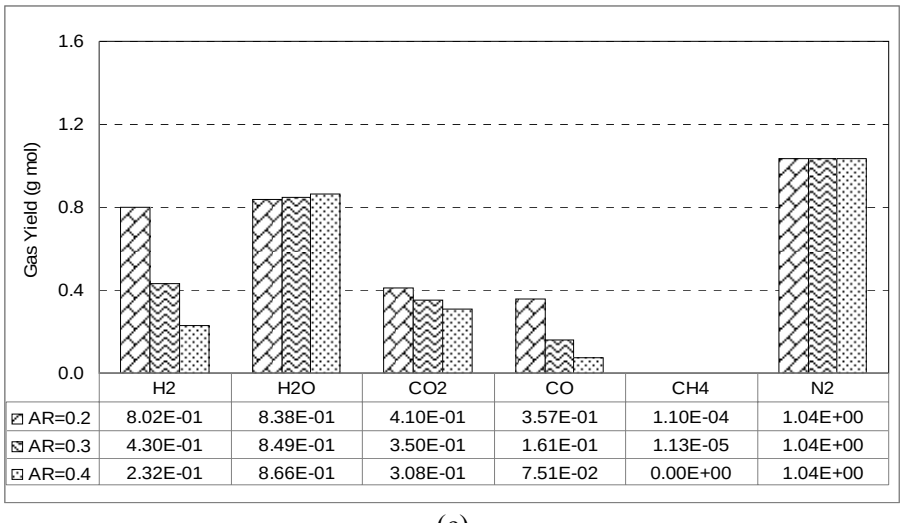

	H2	H2O	CO2	CO	CH4	N2
AR=0.2	8.02E-01	8.38E-01	4.10E-01	3.57E-01	1.10E-04	1.04E+00
AR=0.3	4.30E-01	8.49E-01	3.50E-01	1.61E-01	1.13E-05	1.04E+00
AR=0.4	2.32E-01	8.66E-01	3.08E-01	7.51E-02	0.00E+00	1.04E+00

(c)

Figure 10. Results of simulations of biomass gasification with equilibrium and semi-equilibrium models for rice husk under different gasifying conditions (a) Temperature = 1073 K, Carbon conversion = 100%; (b) Temperature = 1073 K, Carbon conversion = 80%; (c) Temperature = 1073 K, Carbon conversion = 60%

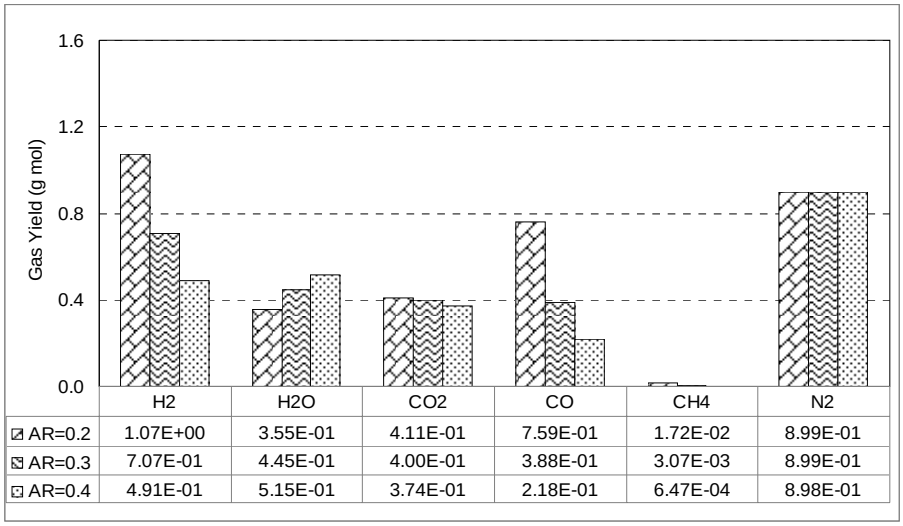

	H2	H2O	CO2	CO	CH4	N2
AR=0.2	1.07E+00	3.55E-01	4.11E-01	7.59E-01	1.72E-02	8.99E-01
AR=0.3	7.07E-01	4.45E-01	4.00E-01	3.88E-01	3.07E-03	8.99E-01
AR=0.4	4.91E-01	5.15E-01	3.74E-01	2.18E-01	6.47E-04	8.98E-01

(a)

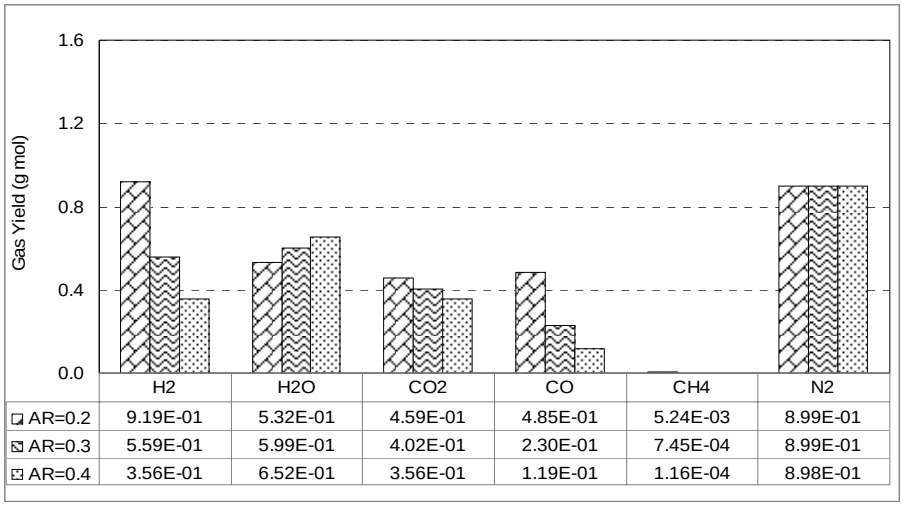

	H2	H2O	CO2	CO	CH4	N2
AR=0.2	9.19E-01	5.32E-01	4.59E-01	4.85E-01	5.24E-03	8.99E-01
AR=0.3	5.59E-01	5.99E-01	4.02E-01	2.30E-01	7.45E-04	8.99E-01
AR=0.4	3.56E-01	6.52E-01	3.56E-01	1.19E-01	1.16E-04	8.98E-01

(b)

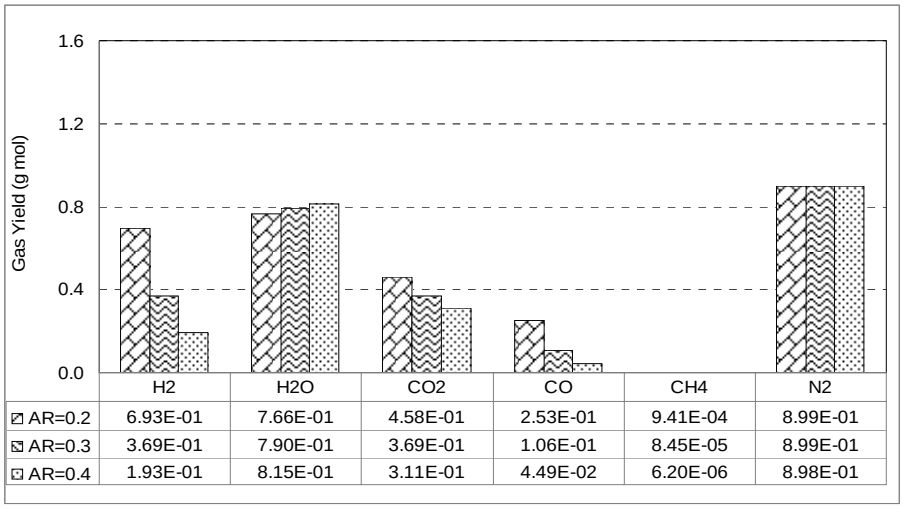

	H2	H2O	CO2	CO	CH4	N2
AR=0.2	6.93E-01	7.66E-01	4.58E-01	2.53E-01	9.41E-04	8.99E-01
AR=0.3	3.69E-01	7.90E-01	3.69E-01	1.06E-01	8.45E-05	8.99E-01
AR=0.4	1.93E-01	8.15E-01	3.11E-01	4.49E-02	6.20E-06	8.98E-01

(c)

Figure 11. Results of simulations of biomass gasification with equilibrium and semi-equilibrium models for wood particles under different gasifying conditions (a) Temperature = 973 K, Carbon conversion = 100%; (b) Temperature = 973 K, Carbon conversion = 80%; (c) Temperature = 973 K, Carbon conversion = 60%

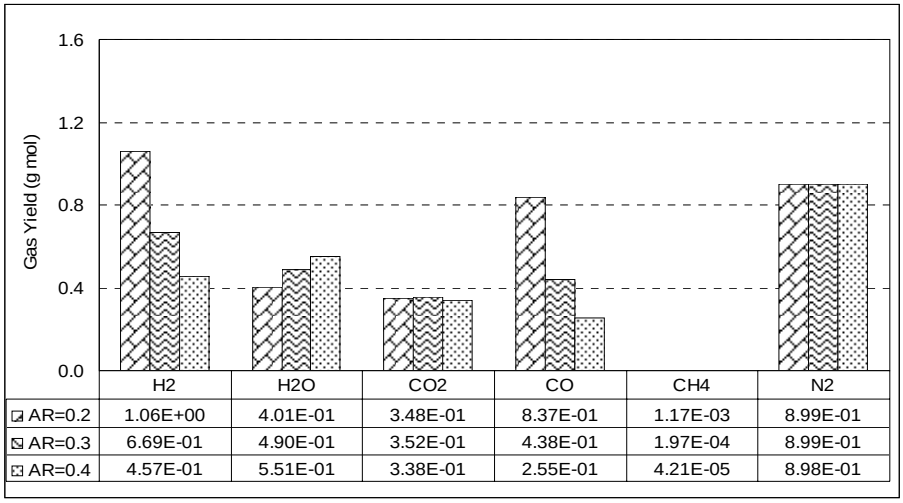

	H2	H2O	CO2	CO	CH4	N2
AR=0.2	1.06E+00	4.01E-01	3.48E-01	8.37E-01	1.17E-03	8.99E-01
AR=0.3	6.69E-01	4.90E-01	3.52E-01	4.38E-01	1.97E-04	8.99E-01
AR=0.4	4.57E-01	5.51E-01	3.38E-01	2.55E-01	4.21E-05	8.98E-01

(a)

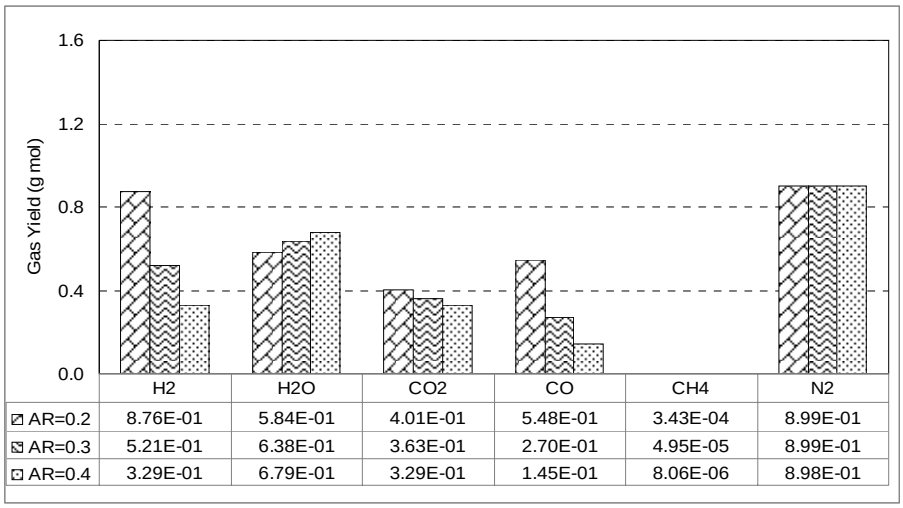

	H2	H2O	CO2	CO	CH4	N2
AR=0.2	8.76E-01	5.84E-01	4.01E-01	5.48E-01	3.43E-04	8.99E-01
AR=0.3	5.21E-01	6.38E-01	3.63E-01	2.70E-01	4.95E-05	8.99E-01
AR=0.4	3.29E-01	6.79E-01	3.29E-01	1.45E-01	8.06E-06	8.98E-01

(b)

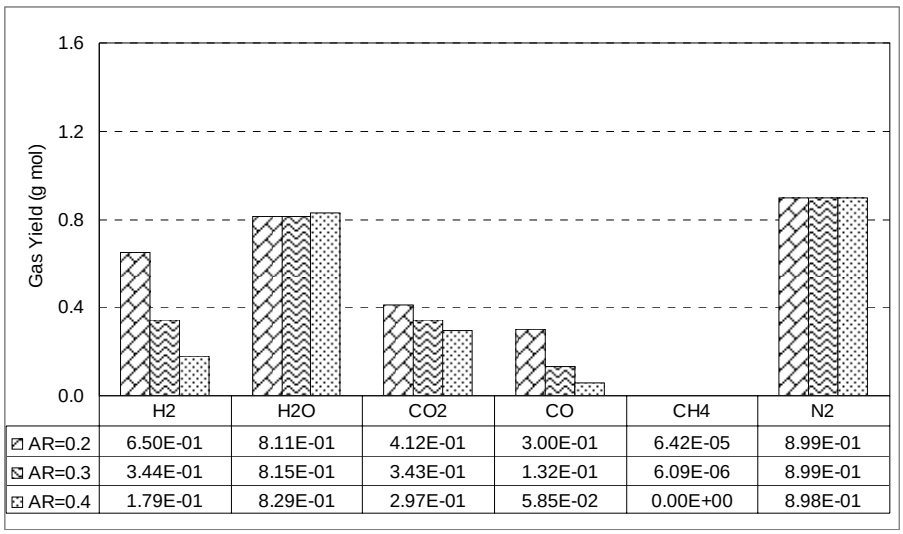

	H2	H2O	CO2	CO	CH4	N2
AR=0.2	6.50E-01	8.11E-01	4.12E-01	3.00E-01	6.42E-05	8.99E-01
AR=0.3	3.44E-01	8.15E-01	3.43E-01	1.32E-01	6.09E-06	8.99E-01
AR=0.4	1.79E-01	8.29E-01	2.97E-01	5.85E-02	0.00E+00	8.98E-01

(c)

Figure 12. Results of simulations of biomass gasification with equilibrium and semi-equilibrium models for wood particles under different gasifying conditions. (A) Temperature = 1073 K, Carbon conversion = 100%. (B) Temperature = 1073 K, Carbon conversion = 80%. (C) Temperature = 1073 K, Carbon conversion = 60%

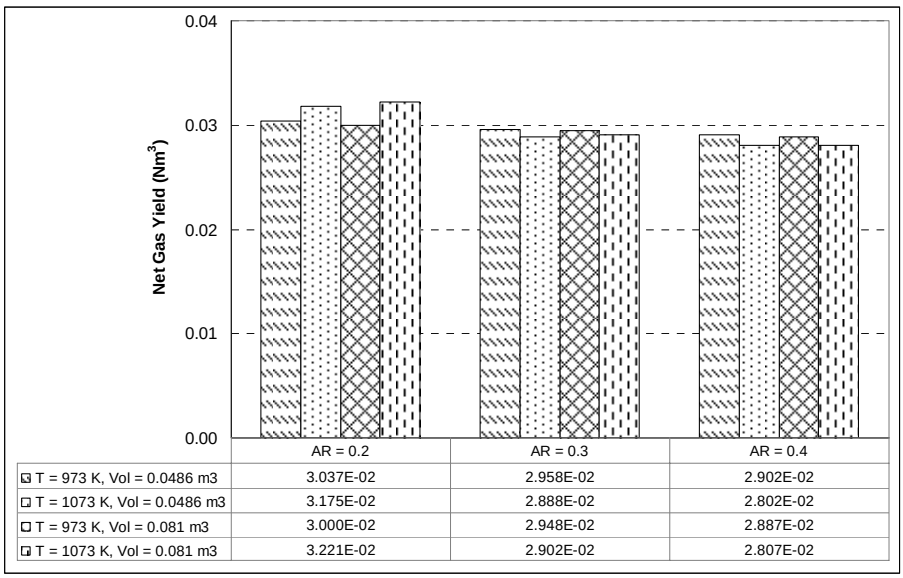

	AR = 0.2	AR = 0.3	AR = 0.4
T = 973 K, Vol = 0.0486 m3	3.037E-02	2.958E-02	2.902E-02
T = 1073 K, Vol = 0.0486 m3	3.175E-02	2.888E-02	2.802E-02
T = 973 K, Vol = 0.081 m3	3.000E-02	2.948E-02	2.887E-02
T = 1073 K, Vol = 0.081 m3	3.221E-02	2.902E-02	2.807E-02

(a)

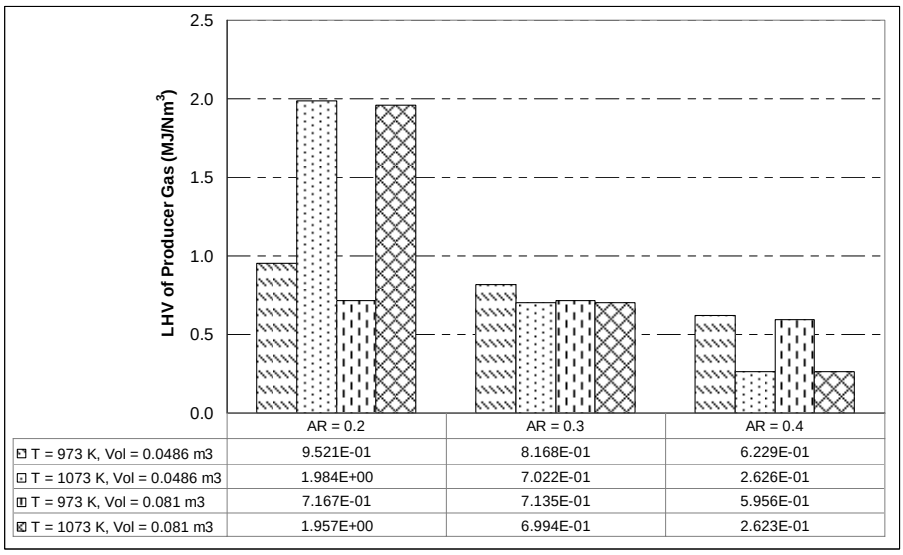

	AR = 0.2	AR = 0.3	AR = 0.4
T = 973 K, Vol = 0.0486 m3	9.521E-01	8.168E-01	6.229E-01
T = 1073 K, Vol = 0.0486 m3	1.984E+00	7.022E-01	2.626E-01
T = 973 K, Vol = 0.081 m3	7.167E-01	7.135E-01	5.956E-01
T = 1073 K, Vol = 0.081 m3	1.957E+00	6.994E-01	2.623E-01

(b)

Figure 13. Results of simulations of biomass gasification with kinetic models: (a) Net gas yield; (b) LHV of the producer gas for different gasification conditions (temperature and carbon conversion) with wood particles as biomass under different gasifying conditions

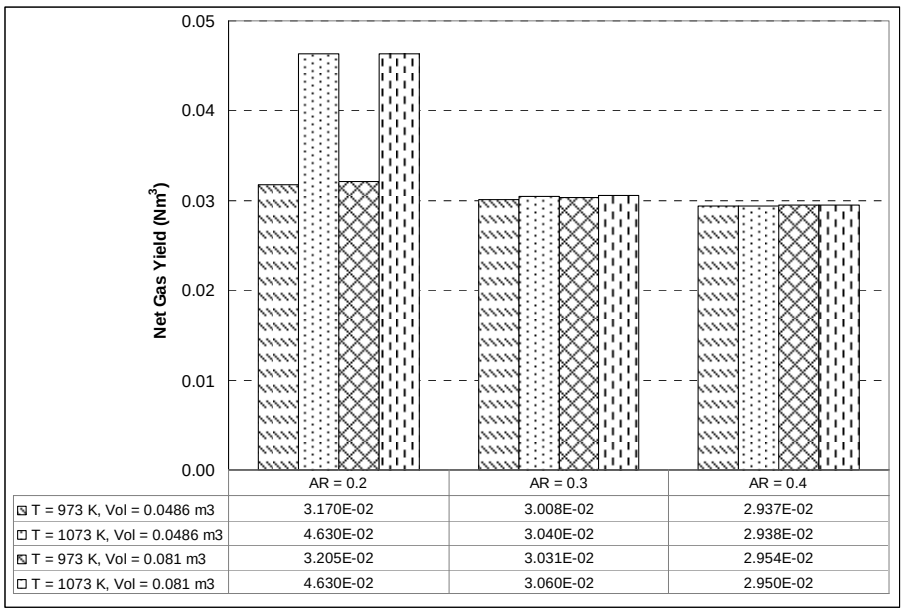

	AR = 0.2	AR = 0.3	AR = 0.4
T = 973 K, Vol = 0.0486 m3	3.170E-02	3.008E-02	2.937E-02
T = 1073 K, Vol = 0.0486 m3	4.630E-02	3.040E-02	2.938E-02
T = 973 K, Vol = 0.081 m3	3.205E-02	3.031E-02	2.954E-02
T = 1073 K, Vol = 0.081 m3	4.630E-02	3.060E-02	2.950E-02

(a)

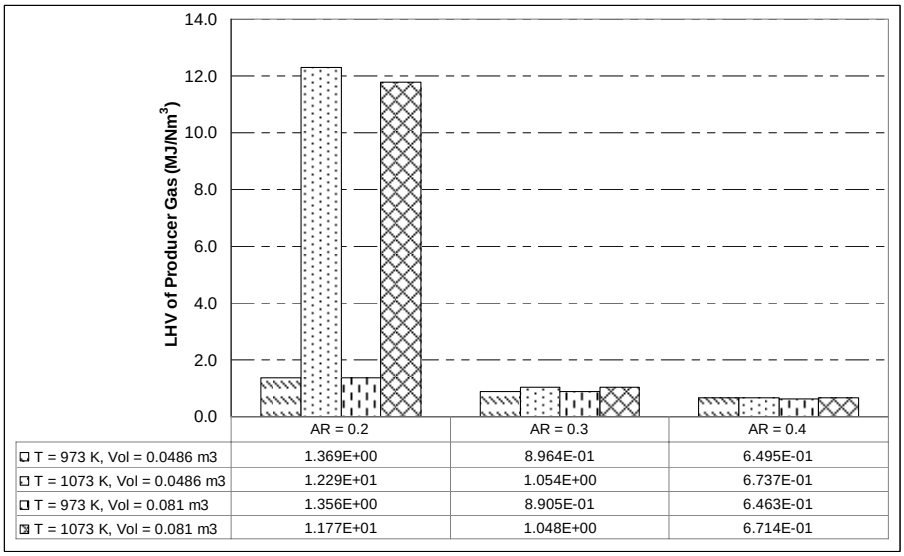

	AR = 0.2	AR = 0.3	AR = 0.4
T = 973 K, Vol = 0.0486 m3	1.369E+00	8.964E-01	6.495E-01
T = 1073 K, Vol = 0.0486 m3	1.229E+01	1.054E+00	6.737E-01
T = 973 K, Vol = 0.081 m3	1.356E+00	8.905E-01	6.463E-01
T = 1073 K, Vol = 0.081 m3	1.177E+01	1.048E+00	6.714E-01

(b)

Figure 14. Results of simulations of biomass gasification with kinetic models: (a) Net gas yield; (b) LHV of the producer gas for different gasification conditions (temperature and carbon conversion) with rice husk as biomass under different gasifying conditions

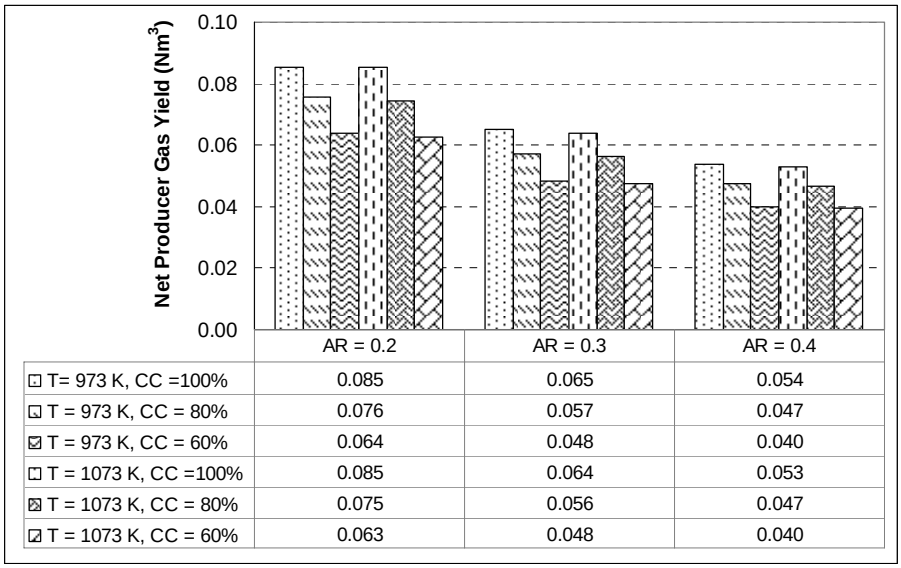

	AR = 0.2	AR = 0.3	AR = 0.4
T= 973 K, CC =100%	0.085	0.065	0.054
T = 973 K, CC = 80%	0.076	0.057	0.047
T = 973 K, CC = 60%	0.064	0.048	0.040
T = 1073 K, CC =100%	0.085	0.064	0.053
T = 1073 K, CC = 80%	0.075	0.056	0.047
T = 1073 K, CC = 60%	0.063	0.048	0.040

(a)

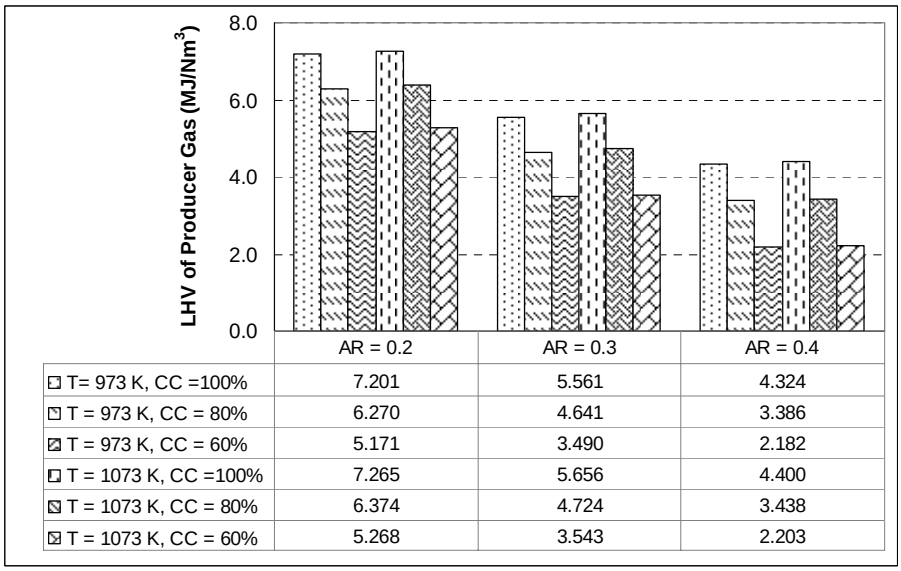

	AR = 0.2	AR = 0.3	AR = 0.4
T= 973 K, CC =100%	7.201	5.561	4.324
T = 973 K, CC = 80%	6.270	4.641	3.386
T = 973 K, CC = 60%	5.171	3.490	2.182
T = 1073 K, CC =100%	7.265	5.656	4.400
T = 1073 K, CC = 80%	6.374	4.724	3.438
T = 1073 K, CC = 60%	5.268	3.543	2.203

(b)

Figure 15. Results of simulations of biomass gasification with equilibrium and semi-equilibrium models: (a) Net gas yield; (b) LHV of the producer gas for different gasification conditions (temperature and carbon conversion) with wood particles as biomass under different gasifying conditions

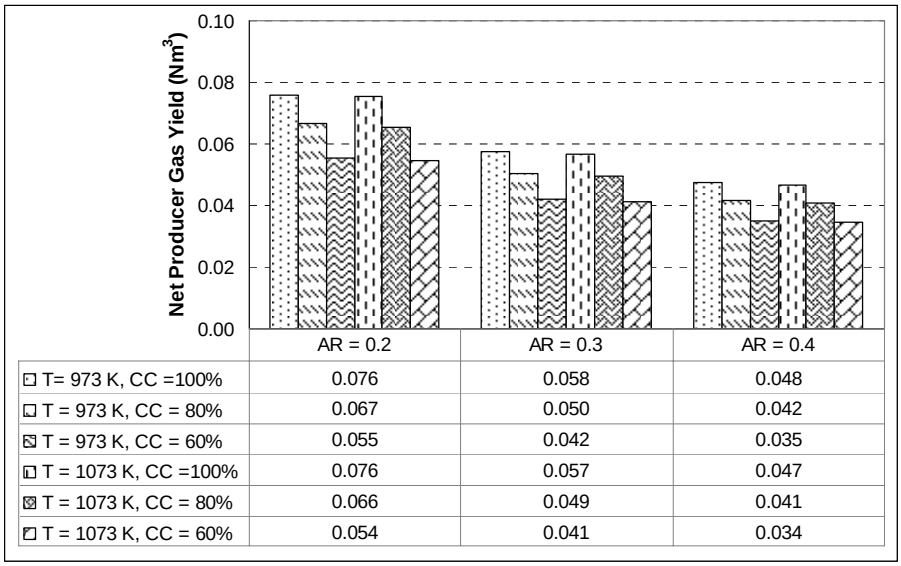

	AR = 0.2	AR = 0.3	AR = 0.4
T= 973 K, CC =100%	0.076	0.058	0.048
T = 973 K, CC = 80%	0.067	0.050	0.042
T = 973 K, CC = 60%	0.055	0.042	0.035
T = 1073 K, CC =100%	0.076	0.057	0.047
T = 1073 K, CC = 80%	0.066	0.049	0.041
T = 1073 K, CC = 60%	0.054	0.041	0.034

(a)

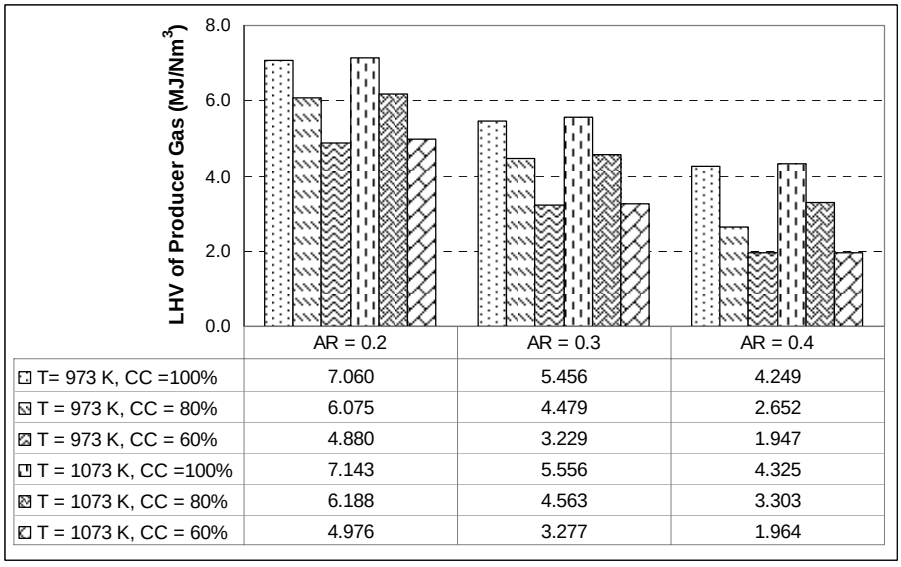

	AR = 0.2	AR = 0.3	AR = 0.4
T= 973 K, CC =100%	7.060	5.456	4.249
T = 973 K, CC = 80%	6.075	4.479	2.652
T = 973 K, CC = 60%	4.880	3.229	1.947
T = 1073 K, CC =100%	7.143	5.556	4.325
T = 1073 K, CC = 80%	6.188	4.563	3.303
T = 1073 K, CC = 60%	4.976	3.277	1.964

(b)

Figure 16. Results of simulations of biomass gasification with equilibrium and semi-equilibrium models: (a) Net gas yield; (b) LHV of the producer gas for different gasification conditions (temperature and carbon conversion) with rice husk as biomass under different gasifying conditions

7. Conclusion

In this paper, we have attempted to present a comparison of equilibrium, semi–equilibrium and kinetic models for biomass gasification. A circulating fluidized bed biomass gasifier has been taken as basis for comparison. Two common biomass, viz. rice husk and wood particles have been used as model biomass. The input for equilibrium and semi–equilibrium model is in terms of an elemental vector, while a stream of 9 species resulting from pyrolysis of biomass forms the input for kinetic models. In semi–equilibrium model, the extent of carbon conversion has been considered as manipulation parameter. Although the trends in molar composition, net yield and LHV of producer gas predicted by the three models under similar conditions of gasification match, there is significant quantitative difference. Carbon conversion achieved in single pass of biomass through the riser of the CFB gasifier is found to be less than the least carbon conversion considered in semi–equilibrium model. Analysis of the kinetic model reveals that formation of significant quantities of char and tar in the biomass pyrolysis, and slow kinetics of gasification /oxidation of these species lead to low per pass carbon conversion, which in turn renders total gas yield and LHV of the gas significantly low. Comparative analysis of the three models has given

an insight into the relative influence of two major operational parameters, viz. temperature and air ratio, on the gasification process. The equilibrium and semi–equilibrium models predict that characteristics of producer gas are relatively insensitive to temperature, while the kinetic model reveals greater sensitivity of producer gas characteristics towards temperature at low air ratios. Another important outcome of the kinetic model analysis is the revelation of effect of gasifier volume. The producer gas composition, yield and LHV have been found to be insensitive to this parameter, i.e. a riser of 6 m height essentially yields producer gas with same characteristics as that from riser of 10 m height. This result gives a strong indication towards optimization of this parameter. Moreover, this result emphasizes on alternative means of enhancing overall carbon conversion through char recycle and catalytic tar oxidation. However, we must also mention that scheme of 13 reactions used in the kinetic model may not include all reactions that could occur in gasification process. Due to this limitation, the actual outcome of the gasification process could differ from predictions of the kinetic model. Secondly, the kinetic model developed in this work is rather system specific in that it has been developed on the basis of a CFB gasifier of specific dimension. If this model is to be applied to other gasifier types or even to a CFB gasifier of different dimensions. We need to make significant changes in it. This is the major limitation of the kinetic model that restricts its versatility.

On a whole, comparative analysis of the equilibrium and kinetic models has highlighted the potential of the equilibrium, semi–equilibrium and models to represent gasification process. Our analysis asserts that equilibrium and semi–equilibrium models could be a useful tool for qualitative assessment / prediction of gasifier performance under different combinations of operating parameters. However, kinetic models provide physically more realistic insight into the various facets of the gasification process and reveal relative influence of various operating and design parameters on the gasification. We believe that results and analysis presented in this paper could be useful for further research in modeling of gasification, and will also give useful guidelines for design engineers for optimization of biomass gasifiers.

Nomenclature

A	cross–sectional area of riser section of the gasifier
a_i	activity coefficient of a species
a_{ij}	number of atoms of the j^{th} element in a molecule of i^{th} substance
b_j	total number of moles of the j^{th} element conveying for biomass particles and turbulent fluidization for sand particles)
C_p	heat capacity at constant pressure
d_p	biomass particle size
d_p^*	non–dimensional particle size (for determination of fluidization regime)
F	molar flow rate of species (formed out of pyrolysis)
G	total Gibbs energy of mixture of species
g_i	chemical potential of a species
H	enthalpy
HP	heat for preheating of the mixture of species
HR	heat of reaction
HT	total heat given to system
l	total number of element
m	total moles of substances in gas phase
P	total pressure of the system
p_i	partial pressure of a species pyrolysis
R	gas constant
$Re_{p,mf}$	particle Reynolds number at minimum fluidizing conditions
r_i	rate of a reaction (subscripts i = 1,…13 indicates reaction number)
s	total moles of substances in condensed or liquid phase
T	temperature of gasification/pyrolysis
t	time
t_d	devolatilization time
u	actual range of velocity for a particular fluidization region
u	velocity of biomass gasification mixture through the riser
u^*	non–dimensional velocity range for a particular fluidization regime (pneumatic
u_{mf}	minimum fluidization velocity

u_t actual terminal settling velocity
u_t^* non–dimensional terminal settling velocity
V volume of gasifier
W weight (or mass) of char particles formed during biomass pyrolysis
x distance coordinate along axis of the riser
X total no of moles in the gas phase
x_i mole fraction of a species *i* in the gasification mixture
y weight fraction (on the basis of moisture free biomass) of the species formed from

Greek letters
φ_s shape factor
ρ density

Subscripts and Superscripts
^{o} standard conditions
^{g} gas phase
^{c} condensed (or liquid) phase
* initial mixture
$_{298}$ at temperature of 298 K
$_f$ formation

References

[1] Eriksson G. Thermodynamic studies of high temperature equilibria – XII: SOLGASMIX, A computer program for calculation of equilibrium composition in multiphase systems. Chem. Scr. 1975, 8, 100–103.
[2] Rhinehart R.R., Felder R.M., Ferrel J.K. Dynamic modeling of a pilot scale fluidized bed coal gasification reactor. Ind. Eng. Chem. Res. 1987, 26, 738–745.
[3] Ciesielzyk E., Gawdzik A. Non-isothermal fluidized bed reactor model for char gasification taking into account bubble growth. Fuel 1994, 73, 105-112.
[4] Sotudeh-Gharebaagh R., Legros R., Chaouki J., Paris J. Simulations of circulating fluidized bed reactor using ASPEN PLUS. Fuel 1998, 77, 327-337.
[5] Srinivasan R.A., Sriramulu S., Kulasekaran S., Agarwal P.K. Mathematical modeling of fluidized bed combustion. 2. Combustion of gases. Fuel 1998, 77, 1033-1049.
[6] Yan H.M., Heidenreich C., Zhang D.K. Mathematical modeling of bubbling fluidized bed coal gasifier and the significance of "net flow". Fuel 1998, 77, 1067-1079.
[7] Wang Q., Huo Z., Li X., Fang M., Ni M., Cen K. A mathematical model for a circulating fluidized bed (CFB) boiler. Energy 1999, 24, 633-653.
[8] Huilin L., Rushan B., Wenti L., Binxi L., Lidan Y. Computations of a circulating fluidized bed boiler with wide particle size distributions. Ind. Eng. Chem. Res. 2000, 39, 3212-3220.
[9] Kim Y.J., Lee J.M., Kim S.D. Modeling of coal gasification in an internally circulating fluidized bed reactor with draught tube. Fuel 2000, 79, 69-77.
[10] Chen C., Horio M., Kojima T. Numerical simulations of entrained flow coal gasifiers: Part I. Modeling of coal gasifiers in an entrained flow gasifier. Chem. Eng. Sci. 2000, 55, 3861-3874.
[11] Chen C., Horio M., Kojima T. Numerical simulations of entrained flow coal gasifiers: Part II. Effects of operating conditions on gasifier performance. Chem. Eng. Sci. 2000, 55, 3875-3883.
[12] Chejne F., Hernandez J.P. Modeling and simulation of coal gasification process in fluidized bed. Fuel 2002, 81, 1687-1702.
[13] Belleville P., Capart R. A model for predicting outlet gas concentration from a wood gasifier (Thermochemical Processing of Biomass, A. V. Bridgwater, Ed., Butterworths), pp. 217-228, London, UK, 1983.
[14] Chang C.C., Fan L.T., Walawender W.P. Dynamic modeling of biomass gasification in a fluidized bed. AIChE Symp. Ser. 1984, 80(234), 80-90.
[15] Van den Aarsen F.G. Fluidized Bed Wood Gasifier Performance and Modeling. Ph.D. Dissertation, University of Twente, Enschede, Netherlands, 1985.

[16] Corella J., Alday F.J., Herguido J. A model for non-stationary states of a commercial fluidized bed air gasifier of biomass (Biomass for Energy and Industry, vol. 2, G. Grassi, Ed., Elsevier), London, pp. 2804-2809, 1990.
[17] Jiang H., Morey R.V. A numerical model of fluidized bed biomass gasifier. Biomass Bioenerg. 1992, 3, 431-447.
[18] Jiang H., Morey R.V. Pyrolysis of corn cobs at fluidization. Biomass Bioenerg. 1992, 3, 81-85.
[19] Wang Y., Kinoshita C.M. Kinetic model of biomass gasification. Sol. Energy 1993, 51(1), 19–25.
[20] Mansaray K.G., Al–Taweel A.M., Ghaly A.E., Hamdullahpur F., Ugursal V.I. Mathematical modeling of a fluidized bed rice husk gasifier: part I – model development. Energ. Source. 2000, 22(1), 83–98.
[21] Mansaray K.G., Ghaly A.E., Al–Taweel A.M., Ugursal V.I., Hamdullahpur F. Mathematical modeling of a fluidized bed rice husk gasifier: part II – model verification. Energ. Source. 2000, 22(3), 281–296.
[22] Sadaka S.S., Ghaly A.E., Sabbah M.A. Two phase biomass air-steam gasification model for fluidized bed reactors: part I – model development. Biomass Bioenerg. 2002, 22, 439-462.
[23] Sadaka S.S., Ghaly A.E., Sabbah M.A. Two phase biomass air-steam gasification model for fluidized bed reactors: part II – model sensitivity. Biomass Bioenerg.2002, 22, 463-477.
[24] Sadaka S.S., Ghaly A.E., Sabbah M.A. Two phase biomass air-steam gasification model for fluidized bed reactors: part III – model validation. Biomass Bioenerg. 2002, 22, 479-487.
[25] Hammel S., Krumm W. Mathematical modeling and simulation of bubbling fluidized bed gasifiers. Powder Technol. 2001, 120, 105-112.
[26] Jennen T., Hiller R., Koneke D., Weinspach P.M. Modeling of gasification of wood in a circulating fluidized bed. Chem. Eng. Technol. 1999, 22(10), 822-826.
[27] Kersten S.R.A., Prins W., van der Drift A., van Swaaij W.P.M. Experimental fact finding in CFB biomass gasification for ECN's 500 kWth pilot plant. Ind. Eng. Chem. Res. 2003, 42, 6755-6764.
[28] Corella J., Sanz A. Modeling circulating fluidized bed biomass gasifiers. A pseudo–rigorous model for stationary state. Fuel Process Technol. 2005, 86(9), 1021–1053.
[29] Liu H., Gibbs B.M. Modelling of NO and N2O emissions from biomass-fired circulating fluidized bed combustors. Fuel 2002, 81, 271-80.
[30] Liu H., Gibbs B.M. Modeling NH3 and HCN emissions from biomass circulating fluidized bed gasifiers. Fuel 2003, 82, 1591–1604.
[31] Dupont C., Boissonnet G., Seiler J.M., Gauthier P., Schweich D. Study about the kinetic processes of biomass steam gasification. Fuel 2007, 86(1–2), 32–40.
[32] Radmanesh R., Chaouki J., Guy C. Biomass gasification in a bubbling fluidized bed reactor: experiments and modeling. AIChE J. 2006, 52(12), 4258–4272.
[33] Nikoo M.B., Mahinpey N. Simulation of biomass gasification in fluidized bed reactor using ASPEN PLUS. Biomass Bioenerg. 2008, 32(12), 1245–1254.
[34] Rodrigues R., Secchi A.R., Marcilio N.R., Godinho M. Modeling of biomass gasification applied to a combined gasifier–combustor unit: equilibrium and kinetic approaches. Computer–Aided Chemical Engineering. 10th Int Symp Process Syst. Eng. 2009, 27A, 657–662.
[35] Roy P.C., Datta A., Chakraborty N. Modelling of a downdraft biomass gasifier with finite rate kinetics in the reduction zone. Int. J. Energ. Res. 2009, 33(9), 833–851.
[36] Kaushal P., Abedi J., Mahinpey N. A comprehensive mathematical model for biomass gasification in a bubbling fluidized bed reactor. Fuel 2010, 89(12), 3650–3661.
[37] Evans P., Paskach T., Reardon J. Detailed kinetic modeling to predict syngas composition from biomass gasification in a PBFB reactor. Environ. Prog. Sust. Energ. 2010, 29(2), 184–192.
[38] Cousins W.J. A theoretical study of wood gasification processes. New Zealand J. Sci. 1978, 21(2), 175–183.
[39] Denn M.M., Yu W.C., Wei J. Parameter sensitivity and kinetics–free modeling of moving bed coal gasifiers. Ind. Eng. Chem. Fundamen. 1979, 18(3), 286–288.
[40] Kosky P.G., Floess J.K. Global model of countercurrent coal gasifiers. Ind. Eng. Chem. Process Des. Dev. 1980, 19(4), 586–592.
[41] Kovacik G., Oguztoreli M., Chambers A., Ozum B. Equilibrium calculations in coal gasification. Int. J. Hydrogen Energy 1990, 15(2), 125–131.
[42] Shesh K.K., Sunawala P.D. Thermodynamics of pressurized air–steam gasification of biomass. Indian J. Technol. 1990, 28(4), 133–138.

[43] Watkinson A.P., Lucas J.P., Lim C.J. A prediction of performance of commercial coal gasifiers. Fuel 1991, 70, 519–527.
[44] Garcia E.Y., Laborde M.A. Hydrogen production by steam reforming of ethanol: thermodynamic analysis. Int. J. Hydrogen Energy 1991, 16(5), 307–312.
[45] Schuster G., Loffler G., Weigl K., Hofbauer H. Biomass steam gasification – an extensive parametric modeling study. Bioresour. Technol. 2001, 77(1), 71–79.
[46] Zainal Z.A., Ali R., Lean C.H., Seetharamu K.N. Prediction of performance of a downdraft gasifier using equilibrium modeling for different biomass materials. Energ. Convers. Manage. 2001, 42(12), 1499–1515.
[47] Alderucci V. Thermodynamic analysis of SOFC fueled by biomass derived gas. Int. J. Hydrogen Energy 1994, 19(4), 369–376.
[48] Ruggiero M., Manfrida G. An equilibrium model for biomass gasification process. Renew. Energ. 1999, 16, 1106–1109.
[49] Altafini C.R., Wander P.R., Barreto R.M. Prediction of working parameters of a wood waste gasifier through an equilibrium model. Energ. Convers. Manage. 2003, 44, 2763–2777.
[50] Melgar A., Perez J.F., Laget H., Horillo A. Thermochemical equilibrium modelling of a gasifying process. Energ. Convers. Manage. 2007, 48(1), 59–67.
[51] Brown D.W.M., Fuchino T., Marechal F.M.A. Stoichiometric equilibrium modeling of biomass gasification: Validation of artificial neural network temperature difference parameter regression. J. Chem. Eng. Jpn. 2007, 40(3), 244–254.
[52] Vera D., Jurado F., Panopoulos K.D., Grammelis P. Modelling of biomass gasifier and microturbine for the olive oil industry. Int. J. Energ. Res. 2011, 36(3), 355-367.
[53] Saxena S.C., Thomas L.A. An equilibrium model for predicting flue-gas composition of an incinerator. Int. J. Energ. Res. 1995, 19(4), 317–327.
[54] Reynolds W.C. The element potential method for chemical equilibrium analysis: Implementation in the interactive program STANJAN. Technical Report, Stanford University, Stanford, USA, pp. 48, 1986.
[55] Smith W.R., Missen R.W. Chemical Reaction Equilibrium Analysis: Theory and Algorithms, Wiley, New York, 1982.
[56] Bharadwaj A. Gasification and Combustion Technologies of Agro–Residues and Their Application to Rural Electric Power Systems in India. Ph.D. Dissertation, Carnegie Mellon University, Pittsburgh, PA, USA, 2002.
[57] Mahishi M.R., Goswami D.Y. Thermodynamic optimization of biomass gasifier for hydrogen production. Int. J. Hydrogen Energy 2007, 32(16), 3831–3840.
[58] Li X., Grace J.R., Watkinson A.P., Lim C.J., Ergudenler A. Equilibrium modeling of gasification: a free energy minimization approach and its application to a circulating fluidized bed coal gasifier. Fuel 2001, 80, 195–207.
[59] Kersten S.R.A. Biomass Gasification in Circulating Fluidized Beds. Ph.D. Dissertation, University of Twente: Twente University Press, Enschede, Netherland, 2002.
[60] Shand R.N., Bridgwater A.V. Fuel gas from biomass: status and new modeling approaches (Thermochemical Processing of Biomass, A. V. Bridgwater, Ed., Butterworths), pp. 229–254, London, 1984.
[61] Nemtsov D.A., Zabaniotou A. Mathematical modeling and simulation approaches of agricultural residues air gasification in a bubbling fluidized bed reactor. Chem. Eng. J. 2008, 143, 10–31.
[62] Puig–Arnavat M., Bruno J.C., Coronas A. Review and analysis of biomass gasification models. Renew. Sust. Energ. Rev. 2010, 14(9), 2841–2851.
[63] Prakash N., Karunanithi T. Advances in modeling and simulation of biomass pyrolysis. Asian J. Sci. Res. 2009, 2(1), 1–27.
[64] FactWeb. [Online]. Available: http://www.factsage.com, 2011.
[65] Bale C.W., Chartrand P., Degterov S.A., Eriksson G., Hack K., Mahfoud R.B., Melancon J., Pelton A.D., Petersen S. FACTSAGE thermochemical software and databases. Calphad. 2002, 26(2), 189–228.
[66] Buragohain B., Mahanta P., Moholkar V.S. Thermodynamic optimization of biomass gasification for decentralized power generation and Fischer–Tropsch synthesis. Energy 2010, 35, 2557-2579.

[67] Narvaez I., Orio A., Aznar M.P., Corella J. Biomass gasification with air in an atmospheric bubbling fluidized bed. Effect of six operational variables on the quality of the produced raw gas. Ind. Eng. Chem. Res. 1996, 35, 2110–2120.
[68] Mansaray K.G., Ghaly A.E., Al–Taweel A.M., Hamdullahpur F., Ugursal V.I. Air gasification of rice husk in a dual distributor type fluidized bed reactor. Biomass Bioenerg. 1999, 17, 315–332.
[69] Kunii D., Levenspiel O. Fluidization Engineering (2nd ed., Butterworth-Heinemann), Boston, 1992.
[70] Lv P.M., Xiong Z.H., Chang J., Wu C.Z., Chen Y., Zhu J. X. An experimental study on biomass air–steam gasification in a fluidized bed. Bioresour. Technol. 2004, 95, 95–101.
[71] Cao Y., Wang Y., Riley J.T., Pan W.P. A novel biomass air gasification process for producing tar–free higher heating value fuel gas. Fuel Process Technol. 2006, 87, 343–353.
[72] Zhao Y., Sun S., Tian H.M., Qian J., Su F.M., Ling F. Characteristics of rice husk gasification in an entrained flow reactor. Bioresour. Technol. 2009, 100, 6040-6044.
[73] Scott D.S., Piskorz J. The flash pyrolysis of aspen-poplar wood. Can. J. Chem. Eng. 1982, 60, 666-674.
[74] Scott D.S., Piskorz J. The continuous flash pyrolysis of biomass. Can. J. Chem. Eng. 1984, 62, 404-412.
[75] Scott D.S., Piskorz J., Bergougnou M.A., Graham R., Overend R.P. The role of temperature in the fast pyrolysis of cellulose and wood. Ind. Eng. Chem. Res. 1988, 27, 8-15.
[76] Beaumont O., Schwob Y. Influence of physical or chemical parameters on wood pyrolysis. Ind. Eng. Chem. Process Des. Dev. 1984, 23(4), 637-641.
[77] Gray M.R., Corcoran W.H., Gavalas G.R. Pyrolysis of a wood derived material: Effect of moisture content and ash content. Ind. Eng. Chem. Process Des. Dev.1985, 24, 646-651.
[78] Nunn T.R., Howard J.B., Longwell J.P., Peters W.A. Product compositions and kinetics in the rapid pyrolysis of sweet gum hardwood. Ind. Eng. Chem. Process Des. Dev. 1985, 24(3), 836-844.
[79] Kashiwagi T., Ohlemiller T., Werner K. Effects of external radiant flux and ambient oxygen concentration on non-flaming gasification rates and evolved products of white pine. Combust. Flame 1987, 69(3), 331-345.
[80] Chan W.R., Kelbon M., Krieger-Brockett B. Single particle pyrolysis: correlations of reaction products and process conditions. Ind. Eng. Chem. Res. 1988, 27(12), 2261-2275.
[81] Bilbao R., Millera A., Murillo M.B. Temperature profiles and weight loss in the thermal decomposition of large spherical wood particles. Ind. Eng. Chem. Res. 1993, 32, 1811-1817.
[82] Figueiredo J.L., Valenzuela C., Bernalte A., Encinar J.M. Pyrolysis of holm-oak wood: influence of temperature and particle size. Fuel 1989, 68(8), 1012-1016.
[83] Scott D.S., Piskorz J., Radlein D. Liquid products from the continuous flash pyrolysis of biomass. Ind. Eng. Chem. Process Des. Dev. 1985, 24(3), 581-588.
[84] Williams P.T., Besler S. The pyrolysis of rice husk in a thermogravimetric analyzer and static batch reactor. Fuel 1993, 72(2), 151-159.
[85] Janse A.M.C., de Jonge H.G., Prins W., van Swaaij W.P.M. Combustion kinetics of char obtained by flash pyrolysis of pine wood. Ind. Eng. Chem. Res. 1998, 37(10), 3909-3918.
[86] Di Blasi C., Signorelli G., Di Russo C., Rea G. Product distribution from pyrolysis of wood and agricultural residues. Ind. Eng. Chem. Res. 1999, 38, 2216-2224.
[87] Luo C.H., Aoki K., Uemiya S., Kojima T. Numerical modeling of a jetting fluidized bed gasifier and the comparison with the experimental data. Fuel Process Technol. 1998, 55(3), 193-218.
[88] Saito M., Sadakata M., Sakai T. Measurements of surface combustion rate of single coal particles in laminar-flow furnace. Combust. Sci. Technol. 1987, 51, 109-128.
[89] Biba V., Macak J., Klose E., Malecha J. Mathematical model for the gasification of coal under pressure. Ind. Eng. Chem. Process Des. Dev. 1978, 17, 92-98.
[90] Gururajan V.S., Agarwal P.K., Agnew J.B. Mathematical-model of fluidized-bed coal gasifiers. Chem. Eng. Res. Des. 1992, 70, 211-238.
[91] Jensen A., Johnsson J.E., Andreies J., Laughli K., Read G., Mayer M., Baaumann H., Bonn B. Formation and reduction of NOX in pressurized fluidized bed combustion of coal. Fuel 1995, 74(11), 1555-1569.
[92] Jones W.P., Lindstedt R.P. Global reaction schemes for hydrocarbon combustion. Combust. Flame 1988, 73, 233-249.

[93] Fletcher D.F., Haynes B.S., Christo F.C., Joseph S.D. A CFD based combustion model of an entrained flow biomass gasifier. Appl. Math. Model. 2000, 24, 165-182.
[94] Zimont V.L., Trushin Y.M. Total combustion kinetics of hydrocarbon fuels. Combust. Explosion Shockwaves 1969, 5(4), 391-394.
[95] Dryer F.L., Glassman I. High-temperatureoxidation of CO and CH4. Symposium (International) on Combustion 1973, 14(1), 987–1003.

Buljit Buragohain (b. 1978) is currently working as Assistant Professor at Girijananda Chowdhury Institute of Management and Technology (GIMT). He obtained his B.E. (Mechanical Engineering, 2000) and M.Tech. (Energy Technology, 2002) degrees from Dibrugarh University and Tezpur University respectively. Thereafter, he worked as Project Engineer at Indian Institute of Technology Guwahati in Biogas Project sponsored by Ministry of New and Renewable Energy, Government of India. In August 2011 he was awarded Ph.D. by Indian Institute of Technology Guwahati for the thesis entitled "Thermodynamic Optimization of Biomass Gasification".

Sankar Chakma (b. 1985) is a research scholar in Department of Chemical Engineering at Indian Institute of Technology Guwahati. He obtained his B.Tech. in Chemical Engineering from Jadavpur University in 2009 and M.Tech. in Chemical Engineering with specialization of petroleum refinery engineering from Indian Institute of Technology Guwahati in 2011. Currently he is pursuing Ph.D. in the same department. He is a recipient of Ambuja Young Researcher's Award given by Indian Institute of Chemical Engineers.

Peeush Kumar (b. 1988) obtained his B.Tech. in Chemical Engineering from Indian Institute of Technology Guwahati in 2011. he is currently working at Bharat Heavy Electricals Limited (BHEL) at Bangalore.

P. Mahanta (b. 1963) is working as Professor of Mechanical Engineering at Indian Institute of Technology Guwahati, India. He obtained B.Sc.(Engg) and M.Tech. degrees from REC Rourkela and I.I.T. Kharagpur in 1985 and 1993 respectively. After obtaining Ph.D. from I.I.T. Guwahati in 2000, he joined in the mechanical engineering department of I.I.T. Guwahati as a faculty member. Between 2004-2011, he was Head of Center for Energy at I.I.T. Guwahati. His major research interests are in the area of Heat Transfer, Renewable Energy, Thermodynamics and Waste Heat Recovery.

V.S. Moholkar (b. 1972) is currently working as Associate Professor of Chemical Engineering at Indian Institute of Technology Guwahati, India. He obtained his B.Chem.Engg. and M.Chem.Engg. degrees from Institute of Chemical Technology, Mumbai in 1993 and 1996 respectively. He joined I.I.T. Guwahati in May 2004. He is affiliated to Center for Energy at I.I.T. Guwahati and has been working on thermochemical and biochemical conversion of biomass to liquid and gaseous biofuels.

